The Journal of Experimental Biology 211, 613-629
Published by The Company of Biologists 2008
doi:10.1242/jeb.006270

Recruitment in a heterogeneous population of motor neurons that innervates the depressor muscle of the crayfish walking leg muscle

Andrew A. V. Hill and Daniel Cattaert*

Université de Bordeaux,Centre de Neurosciences Intégratives et Cognitives (CNIC), CNRS, UMR 5228, Bâtiment B2 Biologie Animale, Avenue des Facultés, 33405 Talence Cedex, France

*Author for correspondence (e-mail: d.cattaert@cnic.u-bordeaux1.fr)

Accepted 17 December 2007

SUMMARY

According to the size principle the fine control of muscle tension depends on the orderly recruitment of motor neurons from a heterogeneous pool. We took advantage of the small number of excitatory motor neurons (about 12) that innervate the depressor muscle of the crayfish walking leg to determine if the size principle applies to this muscle. We found that in accordance with the size principle, when stimulated by proprioceptive input, neurons with small extracellular spikes were recruited before neurons with medium or large spikes. Because only a small fraction of the motor neurons responded strongly enough to sensory input to be recruited in this way, we extended our analysis to all neurons by characterizing properties that have classically been associated with recruitment order such as speed of axonal conduction and extracellular spike amplitude. Through a combination of physiological and anatomical criteria we were able to identify seven classes of excitatory depressor motor neurons. The majority of these classes responded to proprioceptive input with a resistance reflex, while a few responded with an assistance reflex, and yet others did not respond. Our results are in general agreement with the size principle. However, we found qualitative differences between neuronal classes in terms of synaptic input and neuronal structure that would in theory be unnecessary, according to a strict interpretation of the size principle. We speculate that the qualitative heterogeneity observed may be due to the fact that the depressor is a complex muscle, consisting of two muscle bundles that share a single insertion but have multiple origins.

Key words: cell morphology, electrophysiology, locomotion, posture, reflex, confocal microscopy.

INTRODUCTION

The ability of an animal to control the movement of its limbs precisely requires the fine control of the speed and force of contraction of its muscles. While ballistic movements such as those involved in escape reflexes require maximal force and, therefore, are accomplished by the near synchronous activation of many of the motor units within a given muscle (Desmedt and Godaux, 1977), movements such as stepping during walking or postural adjustments require graded changes in force (Duysens et al., 2000; Zajac et al., 2002; Zajac et al., 2003). The ability of a muscle to contract over a wide range of speed and force arises in part from changes in motor neuron firing rate (Milner-Brown et al., 1973) and in part from the orderly recruitment of motor units (Binder and Mendel, 1990; Henneman and Mendell, 1981; Mendell, 2005; Petrofsky, 1978; Petrofsky, 1981). Motor units that produce slow, weak muscle contractions are recruited early, whereas motor units that produce fast, strong contractions are recruited as needed to produce the appropriate amount of force (Henneman et al., 1974; Henneman, 1990).

Early work by Henneman and his colleagues showed that the recruitment order was strongly correlated with the amplitude of the extracellular spike recorded from the motor axons – neurons with small spikes are recruited before neurons with large spikes (Henneman et al., 1965). These observations lead to the 'size principle', which states that recruitment order is related to an index of the relative size of a motor neuron such as its extracellular spike amplitude or conduction velocity (Bawa et al., 1984). The 'size' of a motor neuron is correlated with a number of pre- and postsynaptic parameters that influence its susceptibility to fire. Since the original formulation of the size principle, many parameters such as motor unit force, unit type (e.g. slow twitch *versus* fast twitch) and fatigability of the neuromuscular junction have been found to co-vary and to be correlated with recruitment order (Zajac and Faden, 1985).

There are many differences between neuromuscular control in invertebrates and vertebrates. For example, in invertebrates skeletal muscles are generally innervated by both excitatory and inhibitory motor neurons and single muscle fibers may receive polyneuronal innervation (Atwood, 1967; Atwood and Dorai Raj, 1964; Bullock and Horridge, 1965; Kennedy and Davis, 1977). Despite these differences, the motor systems of invertebrates and vertebrates appear to share many common characteristics. Although the size principle was originally discovered in vertebrates, it applies equally well to invertebrates. In the crayfish swimmeret system, as the frequency of swimmeret beating increases, the requisite increase in muscle force is mediated by an orderly recruitment of motor neurons (Davis, 1969; Davis, 1971). Similarly in the stick insect, motor neurons that cause slow muscle contraction (slow motor neurons) are recruited earlier during the stance phase of walking than the fast motor neurons (Gabriel et al., 2003).

In the present study, we took advantage of the relatively small size (12 excitatory motor neurons) of a pool of motor neurons innervating the depressor muscle in the crayfish walking leg to determine whether or not the size principle applies to this

population. We first examined recruitment among a subset of motor neurons that reach firing threshold in response to sensory input from a proprioceptive organ (Cattaert and Le Ray, 2001; Clarac et al., 2000; El Manira et al., 1991; Le Ray et al., 1997a; Le Ray et al., 1997b). We found that neurons with small extracellular spikes are more susceptible to fire than motor neurons with medium or large spikes, indicating that there is an orderly recruitment of motor neurons. Since the majority of the motor neurons do not reach firing threshold in response to sensory input, we then classified all the motor neurons using a combination of anatomical and physiological criteria, including properties that have been classically associated with recruitment order such as extracellular spike size and conduction velocity. The data show that there are seven distinct classes of depressor motor neurons. The differences between these classes are not merely quantitative, but qualitative. According to the size principle, quantitative differences in motor neuron size and the strength of synaptic input are necessary to prevent the motor neurons from being activated in lockstep, but qualitative differences are not necessary. Thus, while the depressor motor neurons follow the size principle in general, they exhibit a degree of heterogeneity that is greater than one would predict based on this principle alone. We speculate that the high degree of heterogeneity may be related to the fact that the depressor muscle is complex (it consists of two bundles that share a single insertion but have multiple origins).

MATERIALS AND METHODS

Animals

We studied crayfish *Procambarus clarkii* Girard 1852, which were obtained locally. They were fed carrots and were kept in groups of about 50 in large aquaria maintained at 13–14°C. Experiments were performed on male and female crayfish weighing 25–30 g.

Preparation

Crayfish were anesthetized by placing them on ice. The ventral nerve cord was then removed together with the 5th walking leg and pinned dorsal side up in a Sylgard™ (Dow Corning, Wiesbaden, Germany) lined Petri dish (Fig. 1A). The 4th and 5th ganglia were desheathed to increase the passive diffusion of oxygen from the saline and permit intracellular recordings. The preparation was maintained at 15°C by means of a Peltier cell and was perfused with fresh saline containing (in mmol l^{-1}) 195 NaCl, 5 KCl, 13 $CaCl_2$, 2 $MgCl_2$ and 3 Hepes, adjusted to pH 7.65.

Depressor motor neurons lie within the ipsilateral hemisegment of the 5th thoracic ganglion (Fig. 1B). These motor neurons have neurites located entirely within the neuropil of this hemisegment and have axons that project to the depressor muscle. Proximally, the axons of the depressor motor neurons run through the same nerve as the axons that innervate the posterior levator muscle and the remotor muscle. After the first bifurcation, one branch (which we will refer to as the depressor nerve) leads to the depressor muscle. In addition to the axons of the excitatory depressor motor neurons, this nerve contains an axon of the common inhibitor (an inhibitory motor neuron that projects to all muscle groups). Near its ending the depressor nerve divides multiple times to innervate individual muscle fibers.

Recordings and electrical stimulation

The muscles that control the second joint of the leg (the coxo-basipodite) were dissected out and stainless steel wire electrodes were placed in contact with the corresponding nerves (Fig. 1B). These electrodes were isolated from the saline bath with a Vaseline™/paraffin oil mixture (10:1). The differential extracellular signals were amplified 2000–10 000-fold and filtered (high-pass 30 Hz, low-pass 30 kHz, 50 Hz notch filter) using Grass Instruments AC preamplifiers (West Warwick, RI, USA). The bath solution was grounded using a small silver plate that was chlorided using chlorine bleach. Stimulation of nerves was done using a

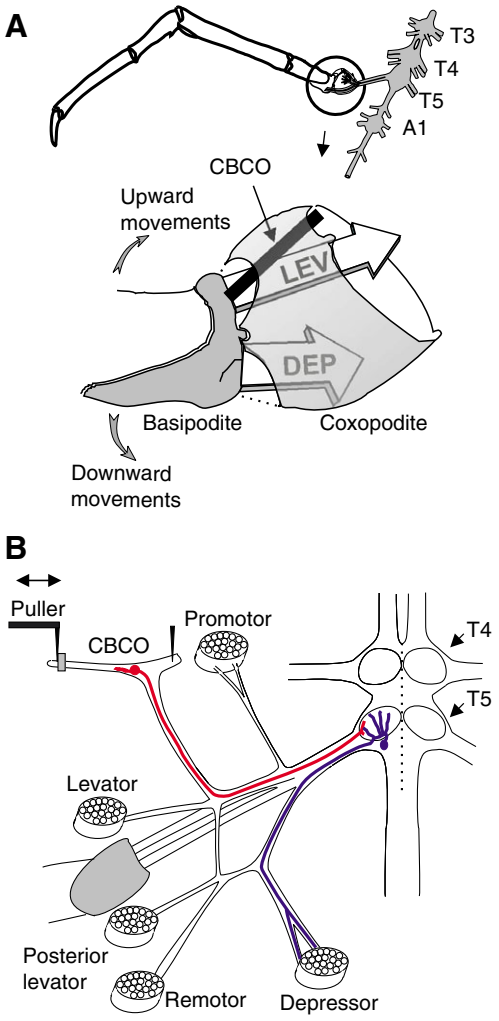

Fig. 1. The *in vitro* walking leg preparation. (A) The 5th walking leg was dissected out together with the 3rd to 5th thoracic ganglia (T3–T5) and the 1st abdominal ganglion (A1) of the ventral nerve cord. In the intact animal the coxo-basipodite chordotonal organ (CBCO) is attached to dorsal edge of the coxopodite and an apodeme at the proximal-dorsal edge of the basipodite. Thus, the tension on the CBCO, which is composed of sensory neurons embedded in an elastic strand, is released during upward movements of the leg and is increased during downward movements. The levator (LEV) and depressor (DEP) muscles are located within the coxopodite. When the depressor muscle contracts, there is a rotation of the basipodite around a pivot point causing the downward movement of the leg and deformation of soft cuticle (dotted line) above and below this point. (B) Extracellular recordings were made from the various motor nerves as well as the sensory nerve of the CBCO (a CBCO neuron is represented in red) using *en passant* electrodes (not shown, see Materials and methods). Intracellular recordings of the motor neurons were made from within the neuropil (a Dep MN is represented in blue). Movements were imposed on the CBCO by a mechanical puller. Stretching the elastic strand mimicked downward movements of the leg, whereas releasing the strand mimicked upward movements. The dotted line marks the midline of the thoracic ganglia.

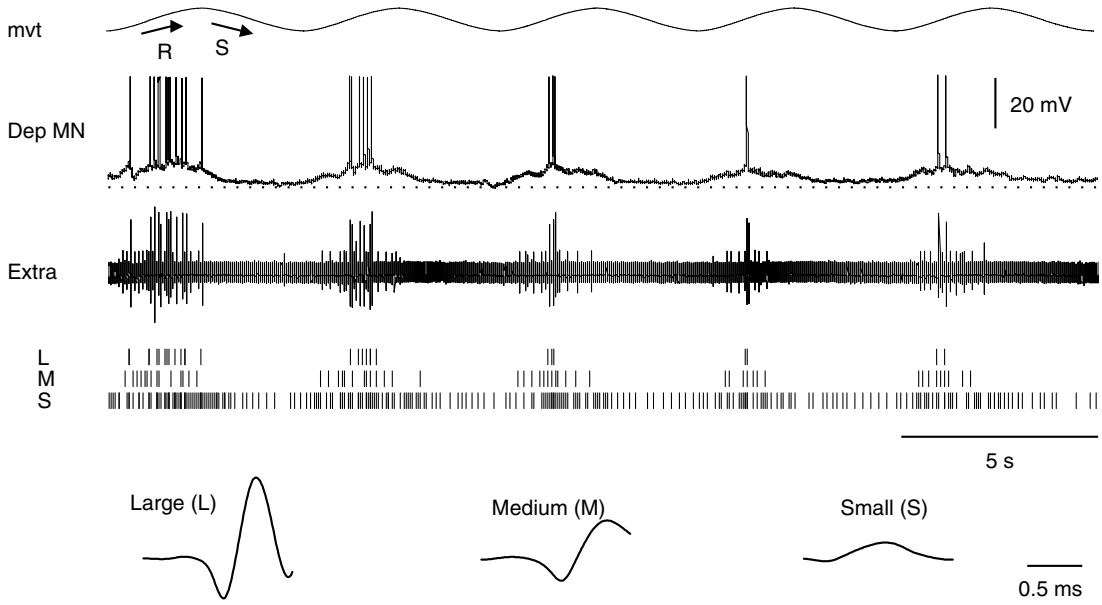

Fig. 2. Recruitment of three motor neurons in response to sensory input. Sinusoidal movements (mvt) were imposed on the CBCO strand while a depressor neuron (Dep MN) was recorded intracellularly from a neuritic branch in the posterior-lateral quadrant of the neuropil (see Fig. 5A for an explanation of quadrants) and extracellular spikes in the depressor nerve were monitored. In the uppermost trace the CBCO strand was stretched (S) and released (R). In this figure and in all subsequent figures an upward deflection of the movement trace corresponds to the release of tension on the CBCO strand, while a downward deflection corresponds to a stretch. The dotted line in the 2nd trace from the top indicates a membrane potential of –65 mV. It was possible to identify three distinct spike shapes in the extracellular record, using a method based on template matching. These spike shapes are shown at the bottom of the figure. A raster plot of the occurrence of these three spike shapes is shown below the raw extracellular record. A short vertical line represents a single spike. Note that the largest extracellular spike (L) corresponds one-for-one with the intracellular spikes.

programmable pulse generator (Master-8, A.M.P.I., Jerusalem, Israel) and a stimulus isolation unit (A.M.P.I.).

Intracellular recordings were made using borosilicate electrodes (1.2 mm o.d. × 0.94 mm i.d., Harvard Apparatus Ltd, Holliston, MA, USA; Brown-Flaming micropipette puller, model P-80, Sutter Instrument Co., Novato, CA, USA) filled with 3 mol l^{-1} KCl (resistance 20 MΩ) and an Axoclamp-2B amplifier (Axon Instruments, Foster City, CA, USA). Signals were monitored using a Yokogawa digital oscilloscope (Tokyo, Japan) and were stored using an analog-to-digital converter and analyzed using Spike2 software (both by Cambridge Electronic Design, Cambridge, UK).

We confirmed that recordings were made from depressor motor neurons either by injecting depolarizing current steps into the main neurite and then recording the time-locked orthodromic extracellular spikes in the depressor nerve or by stimulating the depressor nerve while recording antidromic spikes intracellularly. The extracellular spike waveform was unique for each motor neuron and was quite constant over the course of an experiment; therefore, we were able to identify the spikes of a number of motor neurons based on the shapes of their extracellular spikes. We used a template-matching program included in the Spike 2 software that groups together spikes of similar waveform. There are a number of difficulties with this method. One type of error groups together spikes from two or more neurons that have spikes that are similar in shape; another considers the spikes from a single neuron as coming from two or more neurons. We were aware of these types of errors and each data set was carefully examined by eye to minimize these errors. In addition, in most experiments one-to-one correspondence between extracellular spike shape and the spike of an individual neuron was confirmed by successive intracellular recordings of the majority of the neurons. Orthodromic delay was measured from the peak of the intracellular spike to the first peak or trough of the extracellular spike (spikes were either bi- or triphasic).

Sensory-motor circuit studied

The depressor motor neurons receive sensory input from a proprioceptive organ called the coxo-basipodite chordotonal organ (CBCO). This organ consists of an elastic strand of connective tissue that is attached proximally to the dorsal edge of the coxopodite and distally to the base of an apodeme at the proximal-dorsal edge of the basipodite (Fig. 1A). Embedded within this strand are about 40 sensory neurons that project to the ipsilateral neuropil and make mono- and polysynaptic connections with the depressor motor neurons (El Manira et al., 1991; Le Bon-Jego and Cattaert, 2002). Half of the CBCO sensory neurons are activated when the CBCO strand is stretched, while the other half are activated when the band is released (El Manira et al., 1991). Thus, this proprioceptive organ monitors movements of the limb in the vertical plane. In the *in vitro* preparation a pin holds the proximal end of the CBCO while movements are imposed by a mechanical puller to its distal end (Fig. 1B). In the intact animal, upward movement of the leg releases tension on the CBCO strand whereas downward movement increases tension. Therefore, in the *in vitro* preparation, upward leg movement is mimicked by releasing the tension on the CBCO strand, while downward movement is mimicked by stretching the strand.

The reflex response properties of a depressor neuron were characterized by stretching the elastic strand of the CBCO. The proximal end of the CBCO was pinned to the Sylgard™ dish, while the soft cuticle near the distal end was pinned to a needle, and movements were applied using an electromagnetic puller VT 101 (Ling Dynamic Systems, Meudon-la-forêt, France). To ensure that

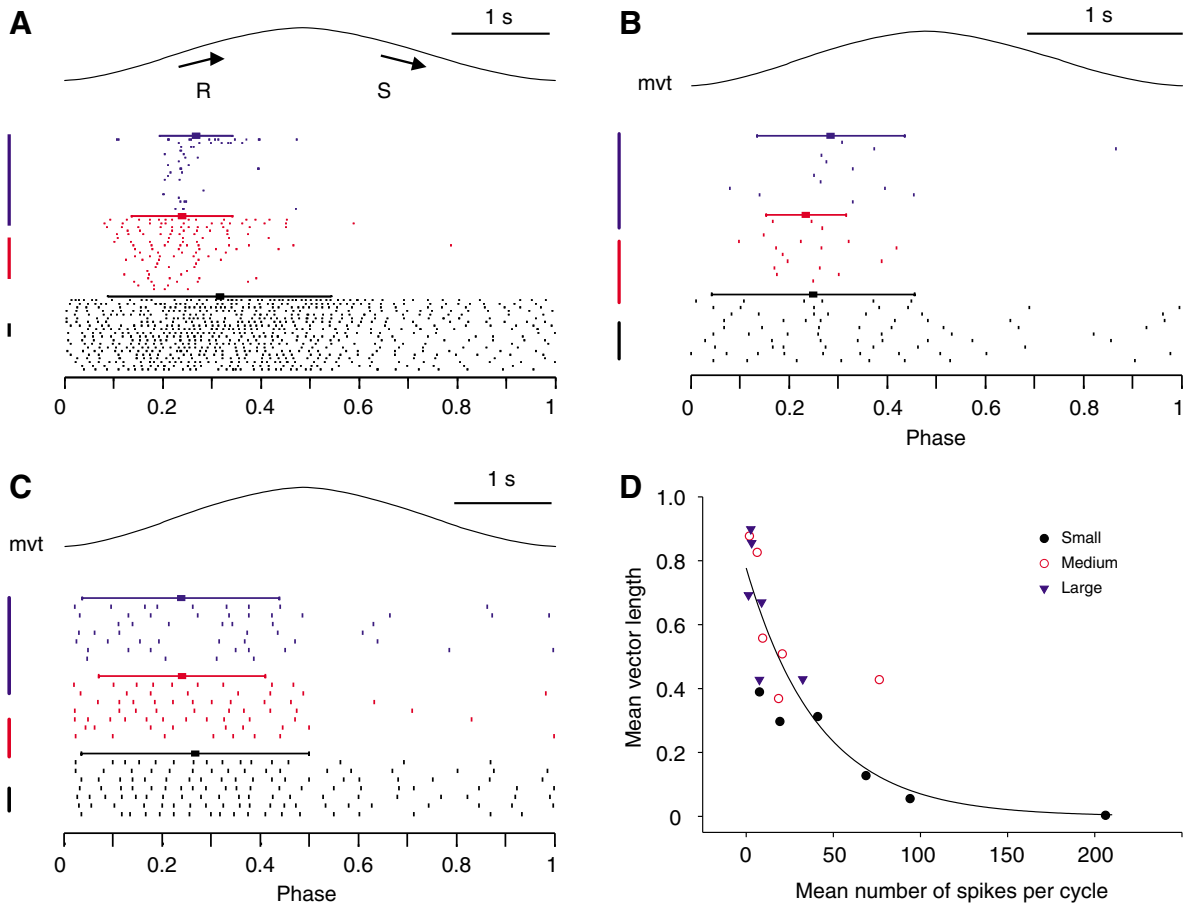

Fig. 3. Spiking timing represented as phase of the sinusoidal movement. (A) Data from the preparation shown in Fig. 2 presented in terms of phase (i.e. a value from 0 to 1 rather than 0° to 360°). (B,C) Data from other preparations. The colored vertical bars show the relative amplitude of the extracellular spikes (large is blue, medium is red, small is black). To the right of each bar are a number of cycles of a raster plot corresponding to that spike. Each row represents one movement cycle with the first cycle on top and subsequent cycles displaced downwards. The small square is the mean spike phase, and the error bars are the standard deviation of this phase (for the calculation of mean spike phase, see Materials and methods). Note that in all three preparations the smallest spike was active through out the entire movement cycle, whereas the medium and large spikes were generally active only during the release phase; however, the mean phases do not differ very much between the different size spikes. (D) The mean vector length, a measure of the degree of clustering of spikes, is correlated with the mean number of spikes per cycle. The mean vector length is highest for neurons that fire very few spikes per cycle. An equation with a single exponential was used to fit the data (R^2=0.718).

the CBCO was not damaged during the dissection, we recorded from the CBCO nerve and only used preparations with robust sensory neuron activity in response to imposed movements of the CBCO strand. In order not to damage the CBCO during the experiment, stretch movements were applied starting from the most released position of the CBCO strand, and the total amplitude of the movement was one third of the released CBCO strand length (1–1.8 mm). The movement control voltage traces were visualized on an oscilloscope and stored on computer.

Sensory input from the chordotonal organ to the depressor motor neurons was also measured in response to electrical stimulation of the CBCO nerve. Monosynaptic and polysynaptic compound EPSPs could be distinguished based on the latency between the stimulus artifact and the onset of the EPSP. IPSPs, if present, were always polysynaptic (Le Bon-Jego and Cattaert, 2002).

Anatomical methods

Neurons were injected with either 5% dextran tetramethylrhodamine (3000 molecular mass, Molecular Probes, Carlsbad, CA, USA) in 0.2 mol l^{-1} potassium acetate, with the electrode shank filled with 2 mol l^{-1} potassium acetate, or 5% Lucifer Yellow (Sigma-Aldrich, St Louis, MO, USA) in distilled water, with the electrode shank filled with 2.5 mmol l^{-1} LiCl. Neurons were injected for 1 h using square-wave pulses (500 ms duration at 1 Hz). Good results were obtained by injecting +10 nA for 5% dextran tetramethylrhodamine and –10 nA for 5% Lucifer Yellow. Ganglia were fixed overnight at 4°C in 4% paraformaldehyde in a 0.2 mol l^{-1} phosphate buffer solution (pH 7.4), dehydrated in series of ethanol solutions of ascending strength (30, 50, 70, 95%, 10 min each; 100%, 2 times, 30 min each), cleared in methyl salicylate (Sigma-Aldrich), and mounted in Permount (Fisher Scientific, Illkirch, France). The ganglia were then imaged using a confocal microscope (Olympus Fluoview BX51, Tokyo, Japan) and the resulting digital images were analyzed using Neurolucida software (MicroBrightField Inc., Williston, VT, USA).

Depressor motor neurons were labeled retrogradely by placing the cut end of the depressor nerve in a pool of 0.5% dextran tetramethylrhodamine (3000 molecular mass, Molecular Probes) in distilled water separated from the surrounding saline solution by

Vaseline™. The preparation was left for 48 h at 4°C and then processed in the same manner as for intracellular injections.

To make nerve cross sections the depressor nerve was dissected out and fixed in 4% glutaraldehyde and 3% paraformaldehyde in sodium cacodylate buffer 0.4 mol l^{-1} at a pH of 7.4 during 18 h at 4°C. Then after rinsing in cacodylate buffer, the nerve was post-fixed in 1% osmium tetroxide. After a second rinsing in cacodylate buffer the nerve was dehydrated in an alcohol series (50%, 75%, 95% and 2×100%; 15 min in each), and embedded in araldite. Semi-thin slices (1 μm thick) were cut with an ultra microtome (Reichert OMU3, Rondebosch, South Africa) and then cleared in toluene and placed on a glass slide. After evaporation (50°C), they were stained with a mixture (50%–50% in volume) of Methylene Blue (1% in sodium borate solution) and Azur Blue (1% in distilled water), then observed under a light microscope and photographed.

Analysis of circular data

The arithmetic mean of circular data is inappropriate to summarize data in which phase values fall near the beginning and end of the linear scale (e.g. the arithmetic mean of 0° and 360° is 180°). Given that θ is the direction and that n is the number of observations and that each vector is of unit length, the solution is to calculate the vector mean direction ($\bar{\theta}$):

$$\bar{\theta} = \arctan(S/C) , \quad (1)$$

where $S=\Sigma\sin\theta$ and $C=\Sigma\cos\theta$. The mean length ($\bar{L}$) of the resulting vector is:

$$\bar{L} = \frac{\sqrt{S^2 + C^2}}{n} , \quad (2)$$

where $\bar{L}$ varies between 0 and 1. The closer the value is to 1 the closer the data are clustered in terms of θ. In Fig. 3 another measure of the variance, the standard deviation, is shown. This value was calculated as the standard deviation of the distance between each θ and $\bar{\theta}$ with the maximum possible distance being 180°. All phase values are expressed as being between 0 and 1 rather than 0° to 360°.

Statistical methods

The significance of differences between groups was determined using a one-way analysis of variance (ANOVA). Pairwise multiple comparisons were done with the Tukey test. P values <0.05 were considered to be significant. All error bars represent the standard deviation (± s.d.).

RESULTS

Recruitment of depressor motor neurons

The first question we wished to address was whether or not the depressor motor neurons are recruited in an orderly fashion in response to sensory input due to movement of the CBCO (see Fig. 1 and Materials and methods). For this purpose we selected a subset of preparations in which at least three motor neurons responded to this sensory input by spiking. Note that all the experiments used in the present study displayed a rather low level of activity. In these experiments, we did not perfuse muscarinic agonists and no spontaneous rhythm, corresponding to forward or backward walking, was observed (Chrachri and Clarac, 1990). In the absence of muscarinic agonists the *in vitro* preparation is in a postural mode (Le Ray and Cattaert, 1997). In this mode only a few preparations presented no spontaneous activity (n=9/33), but in most cases (n=24/33) one unit with a small amplitude extracellular spike fired tonically. Imposed movements of the CBCO strand generally activated from 1 to 3 motor neurons (n=28/33). As described below, most of these active neurons showed a resistance reflex; however, occasionally neurons showing the opposite response, an assistance reflex, were observed. The activity pattern of these neurons is similar to that of the resistance neurons except for the shift in phase (Le Ray and Cattaert, 1997). In a few preparations (n=5/33), no depressor motor neurons were activated by movement. An example of a preparation in which three units fired during the release phase is shown in Fig. 2. In this preparation an intracellularly recorded depressor neuron receives a compound EPSP during the release phase of the movement and fires spikes. This response may be classified as a resistance reflex because *in vivo* a release of tension on the CBCO would correspond to an elevation of the leg, and the spikes fired by the depressor motor neuron would aid in counteracting this movement. The spikes of the intracellularly recorded depressor motor neuron correspond one-for-one with the largest amplitude spike in the extracellular trace. The correspondence between the intracellular spikes and extracellular spikes was further confirmed by the injection of depolarizing current pulses to elicit intracellular spikes that gave rise to extracellular spikes in the depressor nerve with a constant latency from (data not shown). In addition to the largest extracellular spike, it was also possible to find a medium spike and small spike that could be reliably identified as belonging to individual neurons. These extracellular spikes could be distinguished from other spikes of similar amplitude based on a method of template matching (see Materials and methods). Only spikes that are close in waveform to an averaged waveform (template) are considered to belong to the same neuron (the templates found in this experiment for the large, medium, and small amplitude spikes are shown at the bottom of Fig. 2). In the raster plot in the middle of Fig. 2 the occurrence of large, medium and small spikes is indicated by small vertical bars. Note that the neurons are recruited in an orderly manner. The smallest spikes occur throughout the entire cycle of movement with the greatest density of spikes during the release phase of the movement. The medium and large spikes occur almost exclusively during the release phase.

To quantify this type of data we made raster plots in which depressor motor neuron spike times were expressed in terms of phase of the movement stimulus. Examples from three different animals are shown in Fig. 3. In these examples, although the smallest spike occurs throughout each movement cycle, the mean phase occurs during the release phase of the imposed movement (see Materials and methods for the calculation of mean spike phase and s.d.). In contrast, the medium and large spikes are generally less active throughout the cycle, with the mean phase also occurring during the release phase and the majority of spikes occurring during the release phase.

To test the idea that neurons that fire more spikes tend to have their spikes spread out throughout the movement cycle (i.e. small spikes), whereas neurons that fire fewer spikes have spikes that are more tightly clustered (i.e. medium and large spikes) we plotted the mean vector length against the mean number of spikes for 18 neurons from six preparations (Fig. 3D). The mean vector length is a measure of the degree to which the phases of all spikes of a neuron are similar. If one imagines each spike to be represented by a phase value (an angle) and a vector of unit length, then the mean vector length may vary between 0 and 1 with a value of 1 corresponding to spikes that are clustered at a single phase value and a value of 0 arising from either an even

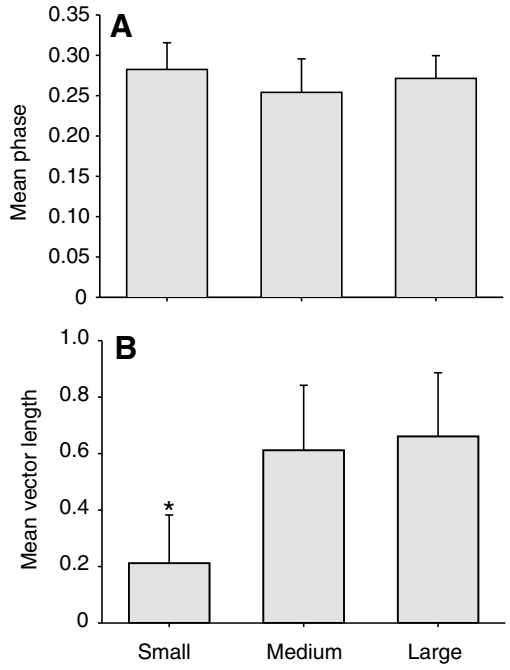

Fig. 4. Mean phase and mean vector length of small, medium and large spikes. Mean phase was calculated as the mean of the mean phases from 5 preparations in which three different sized spikes could be clearly identified as belonging to individual neurons. For an explanation of the calculation of mean vector length see Materials and methods. (A) There was no significant difference between mean phases of small, medium and large spikes. (B) There was a significant difference between the mean vector length of the small spikes and the medium spikes, and between small spikes and large spikes. There was no significant difference between the mean vector length of the medium and large spikes.

distribution of phase values or from clustered phase values that are diametrically opposed (e.g. 0 and 180°; see Materials and methods for details). We found a strong correlation between the mean number of spikes per cycle and the mean vector length (the R^2 value of an exponential fit was 0.718).

In compiled data from five preparations, there was no significant difference between the mean phases of the small, medium and large spikes (Fig. 4). All three types of spikes had mean phase values between 0.25 and 0.30. We found that small spikes have a significantly shorter mean vector length than medium and large spikes, while there was no significant difference between the mean vector lengths of medium and large spikes. Despite large standard deviations, we also found a significant difference in the mean number of spikes per cycle between small spikes (72.8±72.6) and large spikes (9.3±11.7) (n=6). There was no significant difference between the mean number of small spikes and medium spikes (22.2±27.5) or between the mean number of medium spikes and large spikes. Although there is no discrete break in activity of motor neurons with small spikes, they can be considered to be recruited earlier and derecruited later than neurons with medium or large spikes. Thus, the quantification of these data supports the idea of orderly recruitment of depressor motor neurons.

It should be noted that in the examples presented above only a minority of the neurons within the pool of depressor neurons were active. Indeed, as mentioned above, most depressor motor neurons were silent during stimulation of the CBCO by movement. These silent neurons receive excitatory input from the chordotonal organ sensory neurons but were not sufficiently depolarized to reach spike threshold. It is possible that these neurons may also be recruited in an orderly manner, but there is no way to stimulate them strongly enough through sensory input to cause them to spike.

Total number of depressor motor neurons

In the absence of a way to stimulate all depressor motor neurons to reach spike threshold, we decided to classify the depressor motor neuron, based on their anatomical and physiological properties and to characterize parameters that have been classically associated with recruitment order such as extracellular spike amplitude and conduction velocity. We first wished to determine the total number of motor neurons. We used two different techniques. In the first technique, we cut the depressor nerve and placed it in a pool of fluorescent dye (rhodamine dextran) in order to retrogradely label the cell bodies of the depressor motor neurons (see Materials and methods). In the example showed in Fig. 5A, 13 somata were labeled. In compiled data from 14 preparations the mean number

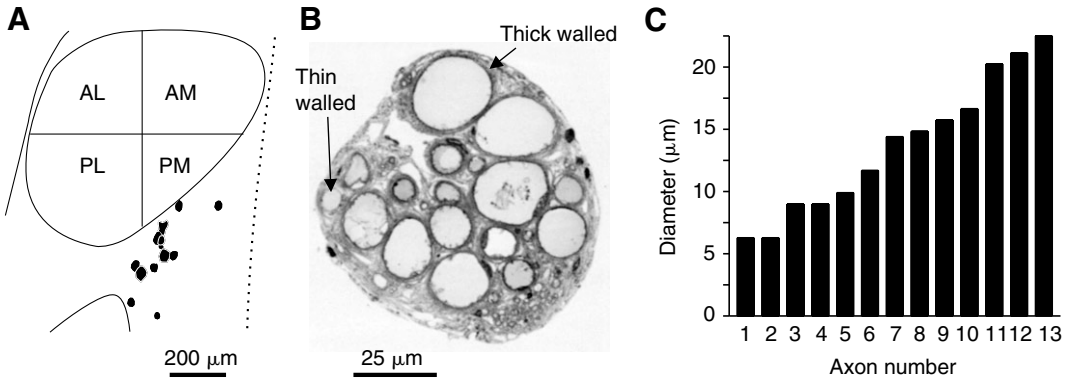

Fig. 5. The somata of the depressor motor neurons lie posterior to the neuropil. (A) Drawing of a rhodamine backfill of the depressor nerve reveals 13 somata (filled circles). For clarity only the somata are shown. The dotted line indicates the midline of the 5th thoracic ganglion. To aid the discussion of anatomical figures that follow, we divided the neuropil into four quadrants: AL (anterior-lateral), AM (anterior-medial), PL (posterior-lateral) and PM (posterior-medial). The cell body of the common inhibitor, which lies on the midline, was not filled in this particular preparation. (B) A cross section of the depressor nerve shows 18 circular profiles, including 13 with thick walls. The five thin-walled profiles are among the smallest in diameter. (C) The diameters of the 13 thick-walled profiles vary in a continuous manner.

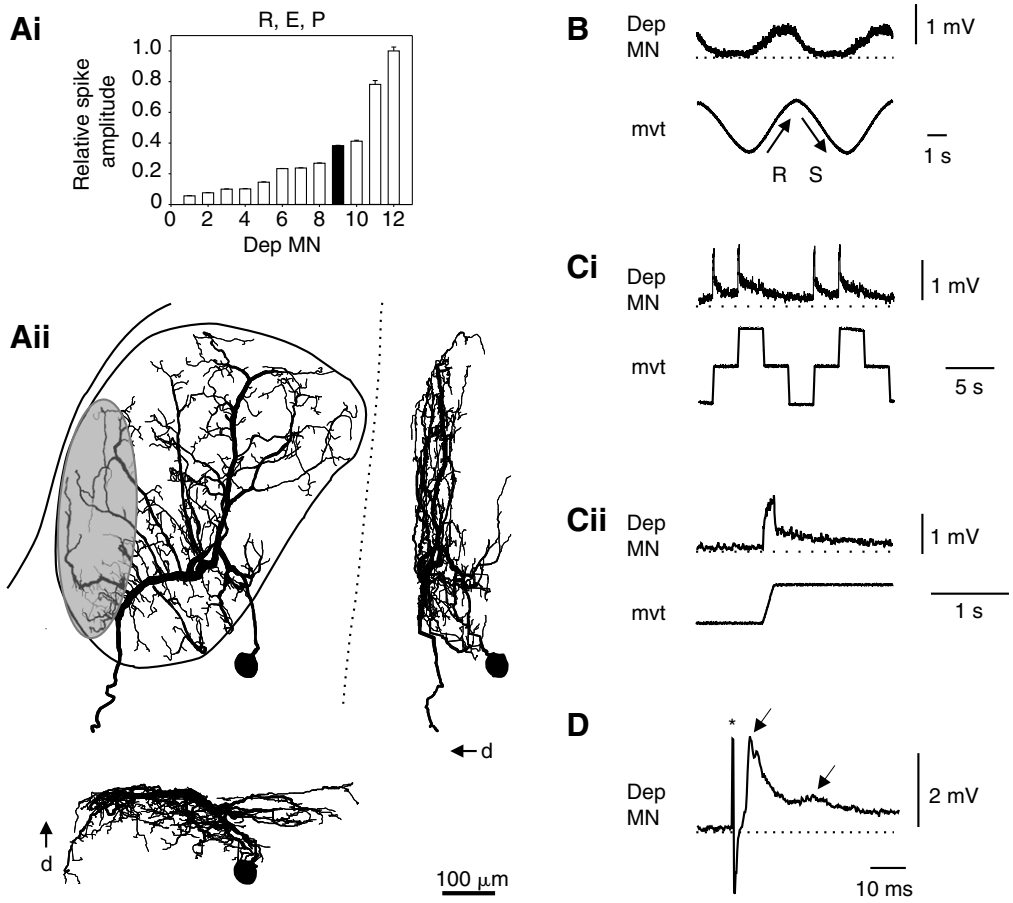

Fig. 6. The anatomical and physiological characterization of an individual depressor motor neuron (Dep MN) that, when viewed from above, has branches that cover the whole neuropil. (Ai) This neuron was recorded from its main neurite, the thick branch in the posterior-lateral quadrant that leads directly to the axon. This depressor motor neuron has the 4th largest extracellular spike of the 12 depressor motor neurons in this experiment. The response properties of this neuron are summarized above the histogram of extracellular spike amplitude. The neuron shows a resistance response (R) to movements imposed on the CBCO strand and receives monosynaptic (E) and polysynaptic (P) excitatory input. (Aii) This neuron is represented from three different viewpoints. Based on previous work describing the anatomy of the CBCO sensory neurons, it may receive monosynaptic input from CBCO sensory neurons in the region indicated by the gray oval (El Manira et al., 1991). In particular, the lateralmost branch, which is also the most ventral, is a likely area of contact. The direction indicated by the arrows is dorsal (d). (B) This neuron depolarizes during the release (R) phase of a sinusoidal movement (mvt) imposed on the CBCO strand. The resting membrane potential, indicated by the dotted line, is –69 mV. The data shown are averages of eight cycles triggered by a timing pulse that was phase locked to the movement trace. (C) A ramp-and-hold stimulus reveals that this neuron is phaso-tonic. It strongly depolarizes during the release phase of ramp movements (Ci; mvt) and also shows a small, slowly decaying depolarization. Note that the ramp movements may appear to be instantaneous (perfectly vertical) at the time scale in Ci but are in fact ramps (Cii). The data shown are averages of eight cycles. (D) Stimulation of the CBCO nerve reveals that this neuron receives mono- and polysynaptic excitatory inputs, which were distinguished based on the delay of the peaks of the compound EPSPs from the stimulus artifact marked with an asterisk (5 ms and 22.7 ms, respectively).

of filled cell bodies was 10.2±2.1. It is possible that motor neurons with very small diameter axons may not have been well labeled. Nevertheless, this technique sets the lower limit on the number of depressor motor neurons to be about 13 (the high-end number observed in three backfill experiments). A similar technique using a cobalt dye also gave an estimated number of depressor motor neurons of 13 (El Manira et al., 1991).

To corroborate our data, we used a second technique. We cut and stained thin cross sections of the depressor nerve (see Materials and methods). These cross sections revealed a total of about 18 circular profiles, 13 with thick walls, and five with thin walls (Fig. 5B). The 13 thick-walled profiles had diameters that ranged continuously from 7 to 22 μm (Fig. 5C). They may correspond to the motor neurons that could be readily labeled using the first technique. The five thin-walled profiles generally had small diameters and may not be motor neurons (see Discussion). Therefore, our results confirm that the depressor muscle is likely innervated by 12 excitatory depressor MNs plus the common inhibitor.

Criteria used for classification of depressor motor neurons

Anatomy

To analyze the population of depressor motor neurons in more detail, we impaled them with dye-filled sharp electrodes and recorded their responses to imposed movement of the CBCO strand and to electrical stimulation of the CBCO nerve. A typical experiment is shown in Fig. 6. We impaled a depressor motor neuron in its thick neuritic branch within the posterior-lateral quadrant (see Fig. 5A for an explanation of quadrants). After characterizing the response properties of this neuron, it was filled with rhodamine and its processes were traced from a digital file created with a confocal microscope (see Materials and methods).

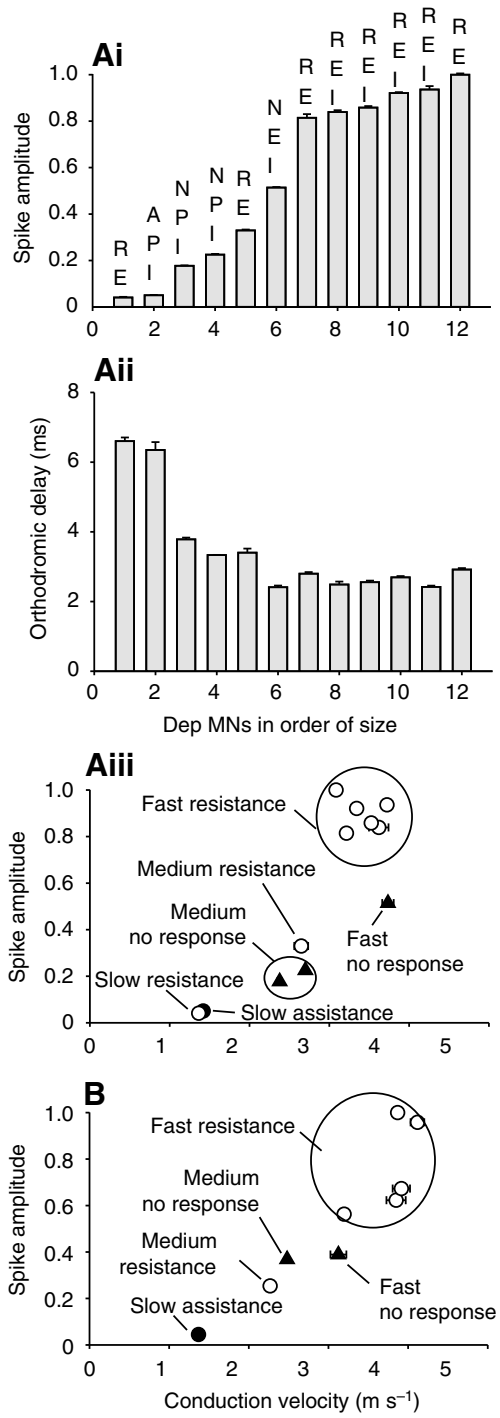

Fig. 7. Two example experiments in which the extracellular spike amplitudes, orthodromic conduction delays and response properties of many depressor motor neurons (Dep MN) were characterized. (A) 12 depressor motor neurons (Dep MN) were characterized. (Ai) The amplitude of the extracellular spike varies continuously. Spike amplitudes were normalized to the largest amplitude found in a given experiment. The neurons showed a resistance (R) reflex, and assistance (A) reflex, or no (N) response to movements imposed on the CBCO strand. Neurons received monosynaptic EPSPS (E), polysynaptic EPSPs (P), and IPSPs (I). (Aii) The neurons with the smallest spikes have the longest orthodromic delays. (Aiii) Conduction velocity was calculated for each neuron by dividing the distance between the neuropil and the site of the extracellular recording (7.5 mm) by the orthodromic delay. Conduction velocity varied with extracellular spike amplitude. (B) In a second experiment, we recorded from nine depressor motor neurons with similar trends to those found in the first experiment.

The neuron was identified unequivocally as a depressor motor neuron by either stimulating the depressor nerve to evoke antidromic spikes or by injecting depolarizing intracellular pulses to evoke orthodromic spikes, and looking for a one-to-one correspondence between intracellular and extracellular spikes (see Materials and methods). We always recorded from neuritic branches within the posterior-lateral quadrant of the neuropil. Since the main neuritic branch within this quadrant leads directly to the axon and the spike initiation zone is presumably located in the proximal axonal segment, the synaptic potentials recorded from this vantage point should be weighted in a manner that accurately represents information that is functionally important.

Extracellular spike amplitude

In the same animal, we also sequentially performed intracellular recording from many other depressor neurons. In this particular experiment, we found a total of 12 depressor motor neurons. These neurons were identified based on the uniqueness of the waveforms of their extracellular spikes and the one-to-one correspondence between these extracellular spikes and intracellular spikes. Fig. 6 shows recordings from the neuron with the 4th largest extracellular spike (Fig. 6Ai). Above the histogram of spike amplitudes the letters 'R, E, P' signify that this neuron receives synaptic input in response to imposed movement of the CBCO strand that is consistent with a resistance (R) reflex, and that in response to electrical stimulation of the CBCO nerve this neuron receives mono- and polysynaptic excitatory input (E and P, respectively). The data supporting this characterization are described below.

Reflex response

This particular depressor motor neuron shows a response that is subthreshold but consistent with a resistance reflex. In response to sinusoidal movements it depolarizes during the release phase and repolarizes during the stretch phase (Fig. 6B). In addition, a ramp-and-hold stimulus protocol was also used (Fig. 6Ci). To make clear that the ramp is truly a ramp and not a step, an expanded view of the ramp-and-hold stimulus and the corresponding neuronal response is shown in Fig. 6Cii. As with the sinusoidal stimulus, the motor neuron depolarizes only during the release phase. The ramp-and-hold stimulus is useful for determining whether the change in membrane potential represents a coding of movement or joint position. This depressor motor neuron appears to receive excitatory postsynaptic potentials (EPSPs) coding mainly for movement, since most of the potential decays immediately after the end of each rapid ramp. There is, however, a small component of the response that is long lasting; therefore, the neuron may be considered to be phaso-tonic. During movement, the membrane potential depolarizes relative to the resting membrane potential (dotted line, Fig. 6B,Ci,Cii). Thus, it is possible to infer that the input to this neuron is primarily excitatory. It is, however, possible that the neuron also receives shunting inhibition with a reversal potential close to the resting membrane potential. In this system, the reversal potential of the IPSPs is –72 mV (Le Bon-Jego and Cattaert, 2002). To account for this possibility we injected constant depolarizing current to increase the driving force of IPSPs, but found no evidence of IPSPs in this depressor motor neuron (data not shown).

To further characterize the synaptic input to each motor neuron, we stimulated the chordotonal nerve electrically. A brief voltage pulse (0.5 ms) was applied to the extracellular electrode normally

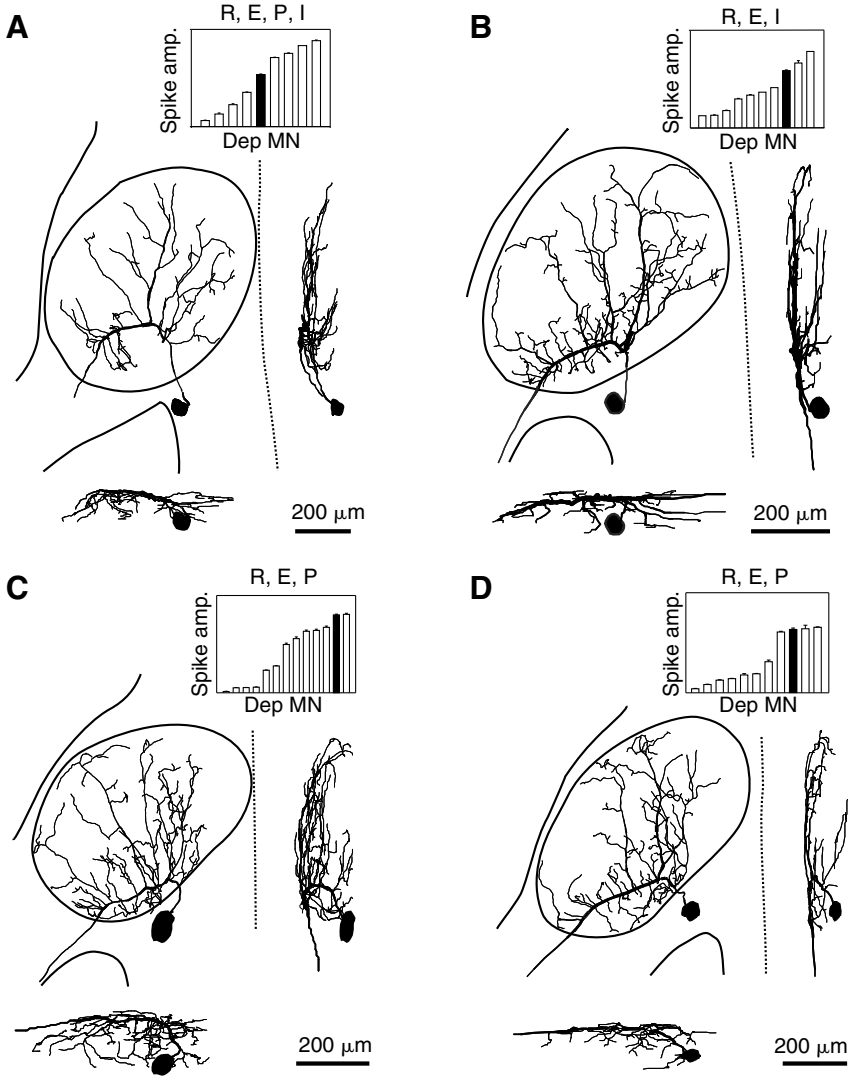

Fig. 8. Four examples of Fast resistance whole neuropil (FR/W) depressor motor neurons (Dep MN) that have neuritic processes extending throughout most of the neuropil when viewed from above. According to our classification scheme, these four neurons (A–D) belong in the same group as the neuron represented in Fig. 6. These neurons have relatively large extracellular spikes (insets), and show a resistance response (R). They receive monosynaptic excitatory (E) input, polysynaptic (P) excitatory input and polysynaptic inhibitory (I) input. Also, similar to the neuron shown in Fig. 6, these neurons presumably receive monosynaptic input on the lateral-most branches in the posterior-lateral quadrant. Note that the neurons in C and D lack medial-most branches. Although it is possible that neurons in C and D may represent another class of neurons, due to the great anatomical and physiological similarity of these neurons with those in A and B and in Fig. 6A, we consider them also to belong to the class FR/W.

used for recording activity of the chordotonal organ (see Materials and methods). In this particular neuron, the response was a compound EPSP with two peaks: one with a latency of 5 ms and another with a latency of 22.7 ms from the stimulus artifact. A delay of 3–12 ms is consistent with a monosynaptic connection, whereas a longer delay is consistent with a polysynaptic connection (El Manira et al., 1991). Therefore, this particular neuron receives both mono- and polysynaptic input. While the large range of delay values given above for a monosynaptic connection may seem unusual, it must be remembered that this delay includes that conduction from the site of nerve stimulation on the sensory nerve as well as the synaptic delay. Thus, monosynaptic connections made by sensory neurons with very small diameter axons may indeed have very long delays. This particular neuron does not receive inhibitory input. Inhibitory input is, however, very common and has been previously established to always be disynaptic (Le Bon-Jego and Cattaert, 2002).

Classes of depressor motor neurons

In a few preparations, we were able to successfully characterize a large number of depressor motor neurons physiologically. Shown in Fig. 7 are the results from two such preparations. We found that there was a large range in extracellular spike amplitude (Fig. 7Ai) and that orthodromic delay varied inversely with the spike amplitude (Fig. 7Ai,Aii). In addition, the conduction velocity, which was calculated based on the distance between the depressor nerve and the neuropil, varied with extracellular spike amplitude (Fig. 7Aiii,B). Assuming that neurons with large amplitude extracellular spikes have axons with large diameters, these results are consistent with the well-known prediction that conduction velocity is proportional to axon diameter (Matsumoto and Tasaki, 1977).

The response of individual neurons to movement of the CBCO strand and to electrical stimulation of the CBCO nerve is summarized in the letters above each bar in the histograms of spike amplitude (Fig. 7Ai). Most neurons showed a resistance response. This is consistent with previously published results. In the *in vitro* preparation the network is most commonly found in a fictive postural mode (standing still) as opposed to a fictive locomotor mode (forwards or backwards walking) (Chrachri and Clarac, 1989). In the postural mode, most motor neurons show a resistance reflex in response to input from the chordotonal organ (El Manira et al., 1991; Le Ray and Cattaert, 1997). However, in each preparation a few neurons were found that showed no response to movement. These neurons tended to have medium sized spikes. Additionally, neurons with small spikes were found that showed an assistance response (they depolarized during the stretch phase). This response is considered an assistance reflex because in the intact animal these neurons would assist a downward deflection on the leg by firing and thereby further enhancing this movement. In the two experiments shown, the assistance neurons have slow conduction velocities and have, therefore, been given the name Slow assistance (SA) motor neurons. However, in other preparations assistance neurons with fast conduction velocities have also been found. Note that in Fig. 7Aiii there is one neuron that is labeled ‘Slow resistance’. This depressor motor neuron has a very slow conduction velocity and a very small extracellular spike amplitude. This slow resistance (SR) motor neuron receives monosynaptic EPSPs, no polysynaptic EPSP and no IPSPs. While

Table 1. Comparison of neuron classes

Neuron class	Number characterized physiologically (anatomically)	Response to movement of CBCO strand	Monosynaptic excitatory input	Polysynaptic excitatory input	Inhibitory input
SA	3(1)	Assistance (*n*=3)	0/3	2/3	2/3
FA	3(2)	Assistance (*n*=3)	3/3	1/3	2/3
MR	4(4)	Resistance (*n*=4)	2/2	1/2	1/2
MNR	3(3)	No response (*n*=3)	0/3	1/3	2/3
FR/W	10(10)	Resistance (*n*=7)	8/8	6/8	3/8
FR/O	6(6)	Resistance (*n*=4)	4/4	0/4	0/4
FNR/O	2(2)	No response (*n*=2)	1/2	0/2	2/2

Numbers are given as the number of positive observations over the total number of observations. For example, FR/W neurons showed polysynaptic excitatory input in 6 out of 8 observations. The total number of observations does not always agree with the number of neurons characterized physiologically for a given neuron class because of experimental difficulties (e.g. loss of an intracellular recording before all tests were performed).
For an explanation of abbreviations, see text and List of abbreviations.

it is possible that this constitutes a class of neurons, no SR neurons were filled; therefore, the anatomy of such SR neurons is not known. We did not attempt any further classification of this type of neuron.

Based on a combination of morphological and physiological criteria, we found that we were able to assign the excitatory depressor motor neurons to seven classes: Fast resistance whole neuropil (FR/W), Fast resistance oblique (FR/O), Fast no response oblique (FNR/O), Medium resistance (MR), Medium no response (MNR), Fast assistance (FA), and Slow assistance (SA).

Fast-resistance depressor motor neurons

The FR neurons may be divided in two classes based on anatomical considerations. The W class includes motor neurons with neuritic branches that fill or nearly fill the whole neuropil (W) when viewed from above, and the O class contains motor neurons with neurites oriented obliquely (O) within the neuropil.

The neuron described above (Fig. 6) belongs to the FR/W class. Four more examples are shown in Fig. 8. The FR/W neurons share many anatomical characteristics. Their main branches are located dorsally. Their secondary neuritic branches extend anteriorly and laterally, and curve downwards, following the contour of the neuropil at its edges. It is in the lateral region of the neuropil that monosynaptic connections may be made from chordotonal sensory neurons (see shaded oval in Fig. 6Aii). Medially, some of these neurons have branches that extend to nearly the midline (*n*=4/10), while others have branches that stop short of the most medial region of the neuropil (*n*=6/10). In Fig. 6 and Fig. 8A,B the neurons have branches that extend to the medial border of the neuropil, while the neurons in Fig. 8C,D do not extend as far medially. In this study, we consider these two types of neurons as simply variants of one class of neuron because their anatomical similarities are so great and because no consistent differences were found in their physiological properties. FR/W neurons show a resistance reflex (*n*=7/7) and receive mono- (*n*=8/8) and polysynaptic (*n*=6/8) EPSPs, as well as IPSPs (*n*=3/8). See Table 1 for a compilation of the response properties of the various classes of neurons.

The FR/W neurons have large extracellular spike amplitudes (75.8±28%) and short orthodromic delays (2.28±0.71 ms). (All values are given as mean ± s.d.) There are a few caveats with regard to the measurement of extracellular spike amplitude and orthodromic delay. First, spike amplitude is presented as a function of the largest spike found in a given preparation. We have attempted to record intracellularly from as many neurons as possible in a given preparation, but it is unlikely that we recorded from all of the neurons. Thus, it is impossible to know with certainty the size of the largest spike. This variation in the size of the largest spike may account in part for the large variation in spike amplitude seen for each group of neurons. In addition, although we used crayfish of a consistent size and always placed the extracellular recording electrode on the depressor nerve in the same location, small variations between animals would cause at least some of the variation in orthodromic delay.

In Fig. 9, one FR/O neuron was filled with rhodamine while another neuron was filled with Lucifer Yellow within the same animal. Despite the great morphological similarity of these two neurons (Fig. 9Ai,Bi,Ci) their synaptic input as measured by stimulation of the CBCO nerve and their responses to sensory input generated by movement of the CBCO strand were very different. The FR/O neuron filled with rhodamine shows a resistance reflex (Fig. 9Bii) and receives monosynaptic input from the sensory neurons (Fig. 9Aii), while the neuron filled with Lucifer yellow has no response to movement (Fig. 9Cii) and receives only inhibitory input in response to electrical stimulation of the CBCO nerve (Fig. 9Aiii). This latter motor neuron was therefore classified as Fast no response oblique (FNR/O). In this study, oblique neurons were filled in eight experiments, and the response to CBCO movement was characterized in six of these experiments. Four of these neurons showed a resistance reflex (FR/O), whereas two showed no response (FNR/O). FR/O neurons received mono-synaptic EPSPs (*n*=4/4), never received polysynaptic EPSPs (*n*=0/4) and never received IPSPS (*n*=0/4). FNR/O neurons sometimes received monosynaptic excitaroy input (*n*=1/2), never received polysynaptic EPSPS (*n*=0/2), and received inhibitory input (*n*=2/2). Similar to the FR/W neurons, the F/O neurons (FNR/O and FR/O taken together) have large extracellular spikes (78.4±24.0%) and short orthodromic delays (2.00±0.48 ms).

Medium motor neurons

Motor neurons with medium (M) amplitude spikes (18.2±2.7%), but orthodromic delays (2.87±1.07 ms) that were short and similar to the delays found in FR/W and F/O neurons could be divided into two classes based on their response to proprioceptive input: ones that responded to synaptic input with a resistance response (MR; *n*=4/7) and ones that had no response (MNR; *n*=3/7). No consistent difference in morphology could be found between these two classes of M neurons. M neurons varied considerably from one another in morphological structure; however, they all have small diameter neuritic branches (*n*=7 dye-fills). Three examples are shown in Fig. 10. One neuron has a sparse arborization (Fig. 10A), another

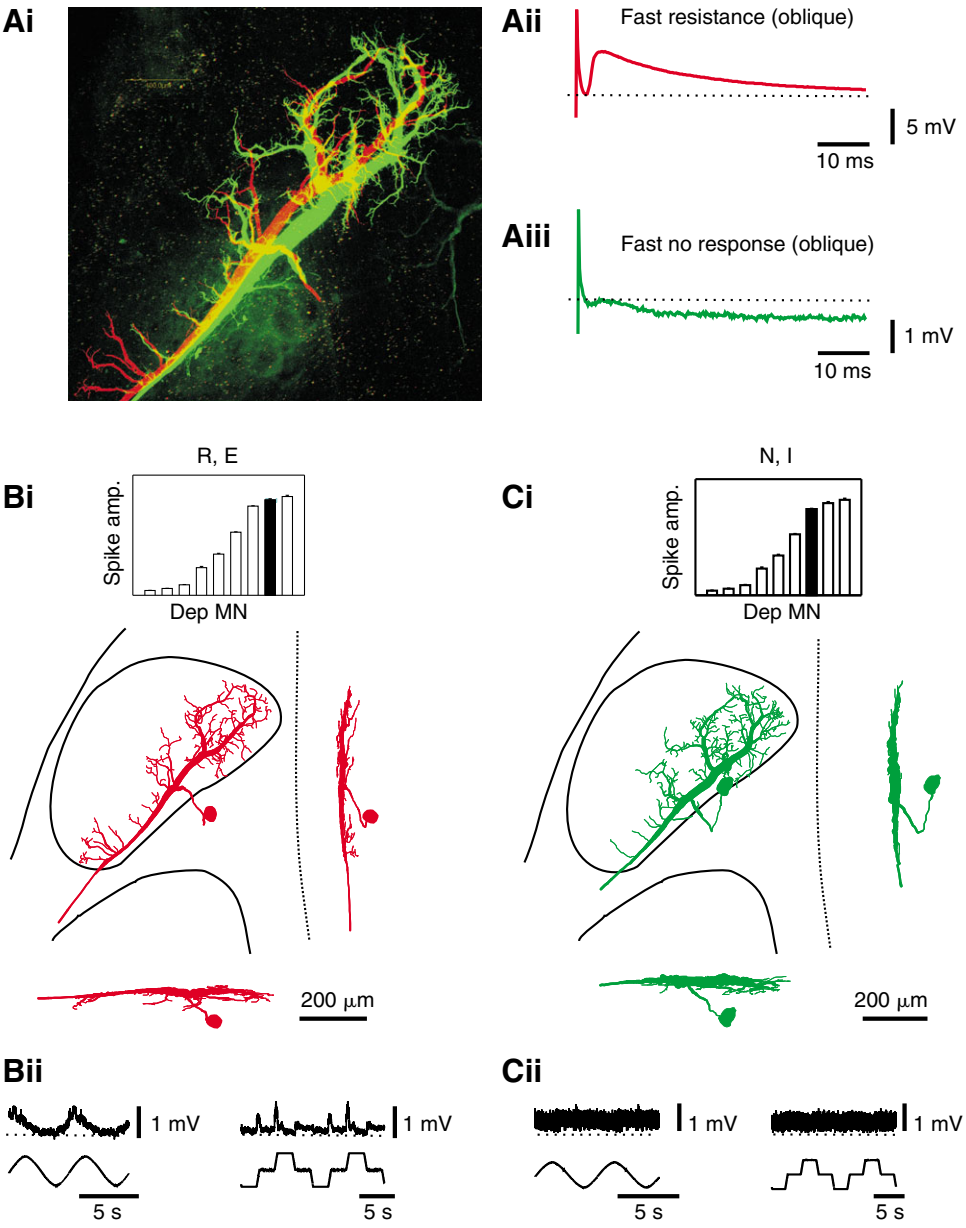

Fig. 9. Two fast oblique (F/O) class depressor motor neurons. These neurons have large diameter main neurites that lie obliquely along the medial edge of the neuropil and a large extracellular spike. (Ai) Two neurons were recorded from and filled with different dyes in a single animal. While there are many similarities in the morphology of the two neurons, there are also some notable differences. For example, the rhodamine-filled neuron (red) has four branches in the lateral-most part of the lateral-posterior quadrant where CBCO sensory neurons may make monosynaptic contact with depressor motor neurons, whereas the Lucifer Yellow-filled neuron (green) has only one branch in this region. (Aii) The rhodamine-filled neuron shows a monosynaptic EPSP with a delay of 5.02 ms from the stimulus artifact and amplitude of 6.08 mV in response to CBCO stimulation (an average of 23 traces is shown). The dotted line indicates a resting membrane potential of –74 mV. (Aiii) The Lucifer Yellow filled neuron shows only an IPSP in response to CBCO stimulation. (Bi) The morphology of the rhodamine-filled neuron. (Ci) The morphology of the Lucifer Yellow-filled neuron. (Bii) The rhodamine-filled neuron showed a resistance response to movement of the CBCO strand. The resting potential was –74 mV. The data shown are averages of 10 cycles triggered off of the movement trace. (Cii) The Lucifer Yellow-filled neuron showed no response to movement of the CBCO strand. The resting potential was –72 mV. The data shown are averages of 11 cycles triggered from the movement trace.

has arborizations that fill nearly the entire neuropil (Fig. 10B), and another lacks branches in the anterior most region of the neuropil (Fig. 10C). The cell body of this third neuron was very anterior compared to those of other depressor motor neurons (cf. Fig. 8, Fig. 10C).

The neuron shown in Fig. 10A was unusual in that it showed a combined resistance/assistance response when stimulated with a ramp-and-hold movement (data not shown). This neuron receives excitatory input during both the release and stretch phase of movement of the CBCO strand. Despite this unusual property we have tentatively grouped this neuron together with other Medium Resistance neurons because its response to sinusoidal input was similar to that of a typical resistance response. As with Fast motor neurons the M neurons also show some specificity of synaptic input. MR neurons receive monosynaptic excitatory input (n=2/2), polysynaptic input (n=1/2), and inhibitory input (n=1/2). MNR neurons do not receive monosynaptic input (n=0/3), but do receive polysynaptic excitatory input (n=1/3) and inhibition (n=2/3).

Assistance motor neurons

In this study we found two classes of depressor motor neurons with an assistance response reflex. Such neurons are depolarized during downward movements of the leg (mimicked by stretch movements of the CBCO strand) and therefore assist the ongoing movement. This class was subdivided into two subclasses, depending on the conduction velocity in the depressor nerve.

The Fast assistance (FA) neurons have small spikes (14.5±0.1%) but short conduction delays (2.13±0.45 ms). This type of assistance neuron was previously described based on intracellular recordings but not dye-fills (Le Ray and Cattaert, 1997). This class of neuron has fine main neurites and some branches in the lateral/posterior region where it may receive monosynaptic contact from the chordotonal sensory neurons (Fig. 11Ai,Bi). These FA neurons receive primarily strong monosynaptic excitatory input during the stretch phase of the movement (Fig. 11Aii,Bii), which corresponds to downward leg movement in the intact animal. They also receive some inhibition during the release phase (Fig. 11Aii,Bii). In three

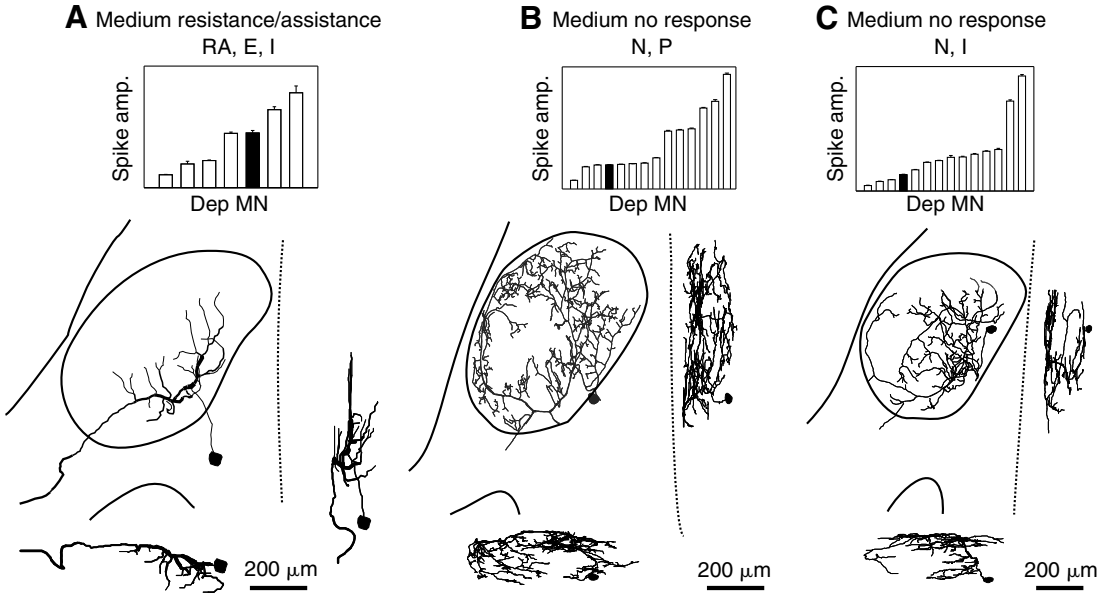

Fig. 10. Three depressor motor neurons (Dep MN) that belong to the Medium (M) class. These neurons have relatively small extracellular spikes, thin neuritic branches and unique branching patterns. Each M neuron that we recorded from was unique in morphology from all other M neurons. (A) This neuron has a relatively sparse neuritic arbor. It shows a resistance and an assistance response to movement (RA), and receives monosynaptic excitatory input (E) and polysynaptic inhibition (I). (B) This neuron has very fine neuritic branches that cover most of the neuropil when viewed from above. It does not respond to movement of the CBCO strand (N) and only receives polysynaptic EPSPs (P). (C) This neuron has neuritic branches that cover most of the neuropil except for the anterior-most parts of the anterior-lateral and anterior-medial quadrants. This neuron shows no response to movement and receives only IPSPs.

preparations, the FA neurons received monosynaptic EPSPs (n=3/3), polysynaptic EPSPs (n=1/3) and inhibition (n=2/3).

The Slow assistance (SA) neurons show long orthodromic conduction delays (see Fig. 7). These neurons have a slow conduction delay (6.17±0.52 ms) and small amplitude extracellular spikes (4.23±0.96%). Because the diameter of the main neurite of this type of neuron was quite small, we were only able to obtain anatomical data from one preparation (physiological data is based on three intracellular recordings). Based on this preparation, however, it appears that this type of neuron has sparse branches and occupies only a small portion of the neuropil (Fig. 12A).

These neurons do not receive monosynaptic EPSPs (n=0/3); although they may receive polysynaptic EPSPs (n=2/3) and IPSPs (n=2/3). In the example shown in Fig. 12, electrical stimulation of the CBCO nerve as well as sinusoidal and ramp-and-hold movements revealed only inhibition (Fig. 12B). The membrane potential of this class of neurons hyperpolarizes during the release phase and depolarizes during the assistance phase. As a result, these neurons act as assistance neurons even though they do not receive monosynaptic EPSPs from the CBCO sensory neurons.

As stated in the Introduction, according to the size principle there are strong correlations between functional properties of a motor neuron, such as their order of recruitment, and properties, such as spike amplitude and conduction velocity. To determine if there are differences between the various classes of motor neurons, we examined compiled data for orthodromic delay and spike amplitude and tested for significant differences between the various classes. For the purpose of these comparisons we condensed the data from the seven different classes into five classes in order to have high enough numbers of neurons in each class to make statistical tests possible (e.g. data for FR/O and FNR/O neurons were combined into one group F/O). We found that the Slow assistance neurons have a longer mean orthodromic delay than all other types of neurons (Fig. 13A), and that the Slow assistance, Fast assistance, and M neurons had significantly smaller extracellular spikes than the FR/W and F/O classes (Fig. 13B).

A number of papers have reported a correlation between physical dimensions of neurons and their recruitment order (Burke et al., 1982; Kovac et al., 1982). We measured soma diameter, neurite diameter and axon diameter for each class of motor neuron and compared them statistically (Fig. 14). The FR/W neurons had significantly larger somata than SA and M neurons (Fig. 14A). The F/O neurons have significantly large diameter main neurites than all other classes of neurons (Fig. 14B). The FR/W and F/O neurons had significantly larger axons than the FA and M neurons (Fig. 14C).

DISCUSSION

Based on the size principle originally proposed by Henneman and his colleagues, the ability of the nervous system to control precisely the movement of a limb depends on the recruitment of motor units of progressively stronger force and greater speed. This hypothesis elegantly simplifies the combinatorial problem of activating a large number of motor units in a smooth and progressive fashion (Henneman et al., 1974; Henneman, 1990). If we make the simplifying assumption that the activation state of a motor neuron is binary (either on or off), then the number of combinations follows the rule 2^n, where n is the number of motor units [see also Henneman et al.'s equation (Henneman et al., 1974; Henneman, 1990)]. It is clear that as the number of motor neurons increases the number of combinations increases very rapidly. With only eight motor units the number of possible combinations of activation is 2^8=256. A system

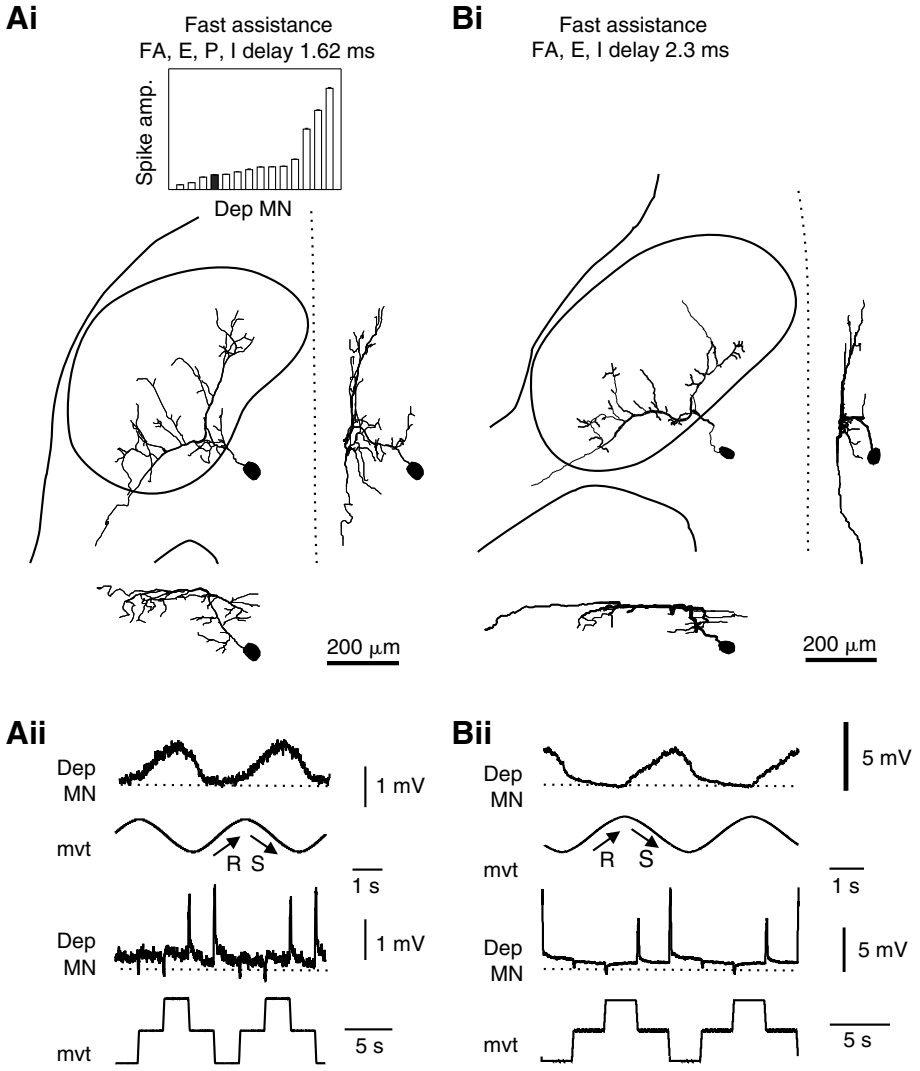

Fig. 11. Two examples of the Fast assistance depressor motor neuron (Dep MN). (Ai) This Fast assistance (FA) neuron has sparse neurites and lacks branches in the anterior-lateral quadrant. It receives mono- (E) and polysynaptic EPSPs (P) as well as IPSPs (I). The orthodromic delay is 1.62 ms. (Aii) The neuron depicted in Ai depolarizes during the stretch phase of sinusoidal movement (mvt). In response to a ramp-and-hold stimulus the neuron strongly depolarizes phasically during stretches and weakly hyperpolarizes during releases. The resting membrane potential (dotted lines) was –69 mV. The response to sinusoidal movement is an average of 9 cycles triggered from the movement trace. The response to ramp-and-hold movement is an average of 5 cycles. (Bi) The morphology of this Fast assistance neuron is similar to that of the one shown to the left. In this particular experiment we did not record from other depressor motor neurons. Therefore, there is no histogram of spike amplitudes. The orthodromic delay is 2.3 ms. (Bii) The response of this neuron to movement is very similar to that of the neuron shown to the left. The resting membrane potential (dotted lines) was –50 mV. The response to sinusoidal movement is an average of 22 cycles triggered from the movement trace. The response to ramp-and-hold movement is an average of 13 cycles.

that allowed 256 possible activation patterns of eight motor units would be unwieldy. If motor units are instead activated in a rank order then the number of combinations is only nine (including the case in which no units are active). Furthermore, if the activation order of motor units is correlated positively with the capacity to generate force, then a full range of muscle contractions may be achieved.

In the present study we found that in the pool of motor neurons that innervate the depressor muscle of the crayfish leg, orderly recruitment occurs in response to sensory input generated by the repetitive activation of a proprioceptive organ. Neurons with small spikes had significantly short mean vector lengths than neurons with medium or large spikes, signifying that their spikes were less strongly clustered in time. In an intact animal, the neurons with small spikes would be activated earlier and turned off later than neurons with larger spikes during a movement. We were unable to extend the analysis of recruitment order to the entire population of depressor motor neurons because a large portion of the population of motor neurons did not reach firing threshold in response to sensory input. Since it was impossible to recruit all the motor neurons, we characterized instead the anatomical and physiological properties of the motor neurons, including various parameters that are associated with recruitment order such as extracellular spike amplitude and conduction velocity.

Identification and number of depressor motor neurons

Using nerve sections of the depressor motor nerve, we found 18 circular profiles, 13 with thick walls and five with thin walls. The five thin-walled profiles are likely not motor neurons. They may be modulatory neurons or sensory projections of unknown origin. The 13 thick-walled profiles are likely to be depressor motor neurons (12 depressor motor neurons plus the common inhibitor). This number corresponds to the maximum number of cell bodies observed after depressor motor nerve backfills and is in accordance with similar observations made in the crab depressor (Bévengut and Cournil, 1990). In most of the experiments designed to perform a maximum of intracellular recordings from depressor motor neurons, we found between 12 and 14 profiles of spike shapes recorded in the depressor motor nerve. (In the one experiment where 14 distinct spikes shapes were found, it is possible that spikes shapes from a single neuron or neurons were erroneously subdivided (see Materials and methods for a full explanation). In summary, we estimate that there are 12 excitatory depressor motor neurons.

Twelve motor neurons may seem like a large number to control a single invertebrate muscle, yet is has been shown that proximal muscles are often innervated by relatively large numbers of motor neurons. The general trend is for a reduction

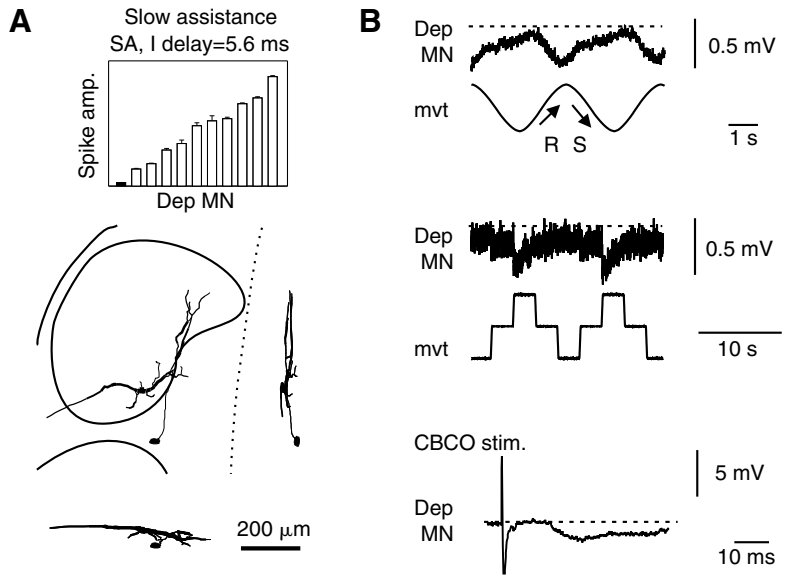

Fig. 12. An example of a Slow assistance (SA) depressor motor neuron (Dep MN). (A) The branches of this neuron are relatively sparse and are restricted to the posterior-medial and anterior-medial quadrants. This neuron receives only polysynaptic inhibition. The orthodromic delay is 5.6 ms. (B) In response to sinusoidal movement (mvt), this neuron hyperpolarized during the release phase and depolarized during the stretch phase, which is consistent with an assistance response. The ramp movement stimuli reveal that the input to this neuron is inhibitory. Similarly electrical stimulation of the CBCO nerve revealed only IPSPs (I). The resting membrane potential indicated by the dotted lines was –55 mV.

in the number of motor neurons per muscle from proximal to distal along the walking leg. Previous studies of the number of motor neurons innervating the two proximal-most joints (four proximal muscles) of the crayfish leg muscles gave 12 depressor, 20 levator, 13 remotor and 20 promotors (Bévengut and Cournil, 1990). The total number of motor neurons that innervate the leg is 90; thus the number of motor neurons (65) that innervate the proximal leg accounts for 2/3 of the total number of motor neurons of the leg (Bévengut and Cournil, 1990). The distal joints have far fewer motor neurons per muscle. For example, the opener muscle is innervated by a single motor neuron. This decrease in motor neurons may reflect and decrease in the complexity of the muscles from proximal to distal (see below for further discussion).

We found that the 12 depressor motor neurons may be divided into seven classes: (1) Fast resistance with an arborization extended through the whole neuropil (FR/W), (2) Fast resistance with an oblique arborization (FR/O), (3) Fast no response with an oblique arborization (FNR/O), (4) Medium resistance (MR), (5) Medium no response (MNR), (6) Slow assistance (SA) and (7) Fast assistance (FA). As described in the Results (Fig. 7A) there may also be a class of slow resistance neurons; however, we have not successfully dye-filled any of these neurons.

The pool of excitatory motor neurons is very heterogeneous; however, we were unable to unequivocally characterize any of the excitatory depressor motor neurons as being unique identified neurons. The one neuron that can be uniquely identified is the common inhibitor. We did not include this neuron in this paper as it has been previously described. This neuron has an extracellular spike of intermediate size and innervates all of the different muscle groups of the leg (Cattaert et al., 1993; Wiens and Wolf, 1993). The main neurite of the common inhibitor lies anteriorly to the primary neurites of all the depressor motor neurons, and its soma lies on the midline of the ganglion, which is in sharp contrast to the somata of depressor motor neurons, which are all located posterior and medial to the neuropil (Chrachri and Clarac, 1989; Elson, 1996). The common inhibitor changes the membrane properties of the muscle fibers to favor rapid relaxation and, thus, promotes more phasic contraction of leg muscles during locomotion (Ballantyne and Rathmayer, 1981). In accordance with this function, it receives excitatory input from the CBCO sensory neurons during both upward and downward movements of the leg (Cattaert et al., 1993).

Response to sensory stimulation

In response to sensory input generated by movement of the elastic strand of the coxo-basipodite chordotonal organ (CBCO) the FR/W, FR/O and MR neurons showed a resistance reflex. Since the *in vitro* preparation is in a postural mode, the resistance reflex would be helpful for maintaining posture in response to changing load, maintaining joint stiffness, and counteracting any forces that would act to change the joint angle such as leg slippage (Barnes, 1977). Two classes of motor neurons, Slow assistance (SA) and Fast assistance (FA), showed assistance reflexes. The role played by the assistance reflex in posture is unknown. However, in vertebrates it has been postulated that subgroups of motor neurons may receive different types of sensory feedback (Duysens, 1989). Furthermore, within the pool of motor neurons that control the proximal-most joint of the leg of the crayfish, both assistance and resistance reflexes were found while the network was in a postural mode (Skorupski et al., 1992).

Specificity of synaptic input

In addition to movement-induced sensory input described above, we also directly stimulated the CBCO nerve electrically. Most classes of motor neurons received mono- and polysynaptic EPSPs and polysynaptic IPSPs; however, there is some specificity of synaptic input. The SA and MNR neurons do not receive monosynaptic EPSPs and the FR/O and FNR/O neurons do not receive polysynaptic EPSPs (see Table 1), in agreement with data from a previous study, showing specificity of synaptic input. Individual sensory neurons make monosynaptic connections with only a subset of motor neurons (Le Ray et al., 1997a). Additionally, some depressor motor neurons show a tonic response to a release-and-hold stimulus while others show a phaso-tonic response (Le Ray et al., 1997a). This difference in response may be due to differences in the synaptic input to these neurons. Some sensory neurons are phasic while others are phaso-tonic (Le Ray et al., 1997a; Le Ray et al., 1997b).

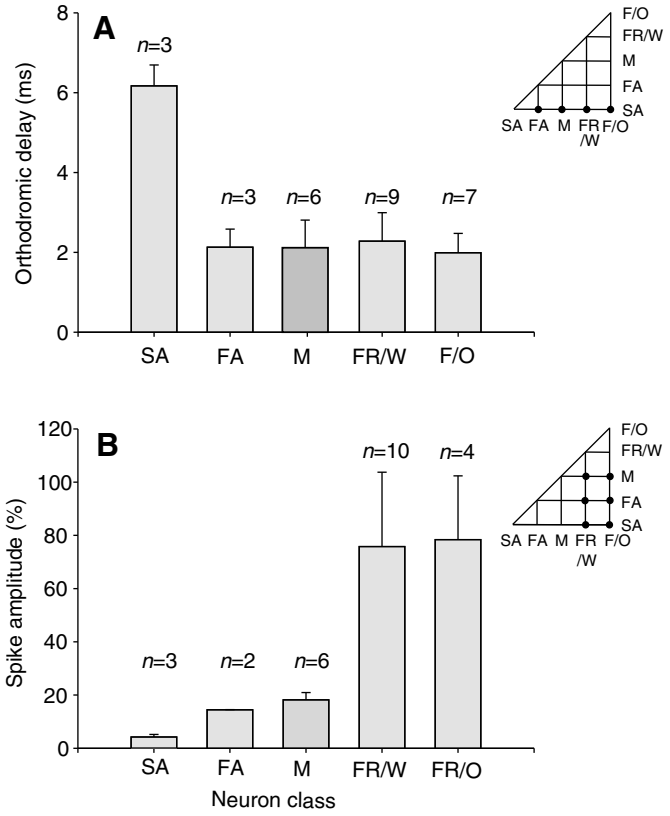

Fig. 13. A summary of extracellular spike amplitude and orthodromic delay for the various classes of neurons. (A) The orthodromic delay of Slow assistance (SA) neurons was significantly different from that of all other classes of neurons. In the inset a solid circle at the intersection of the initials representing each class indicates a significant difference. (B) There were no significant differences in spike amplitude among the Slow assistance (SA) neurons, the Fast assistance (FA) neurons, and the Medium (M) neurons. However, these three classes had significantly different spike amplitudes than the F/O and FR/W classes. There was no significant difference between the F/O and FR/W class neurons.

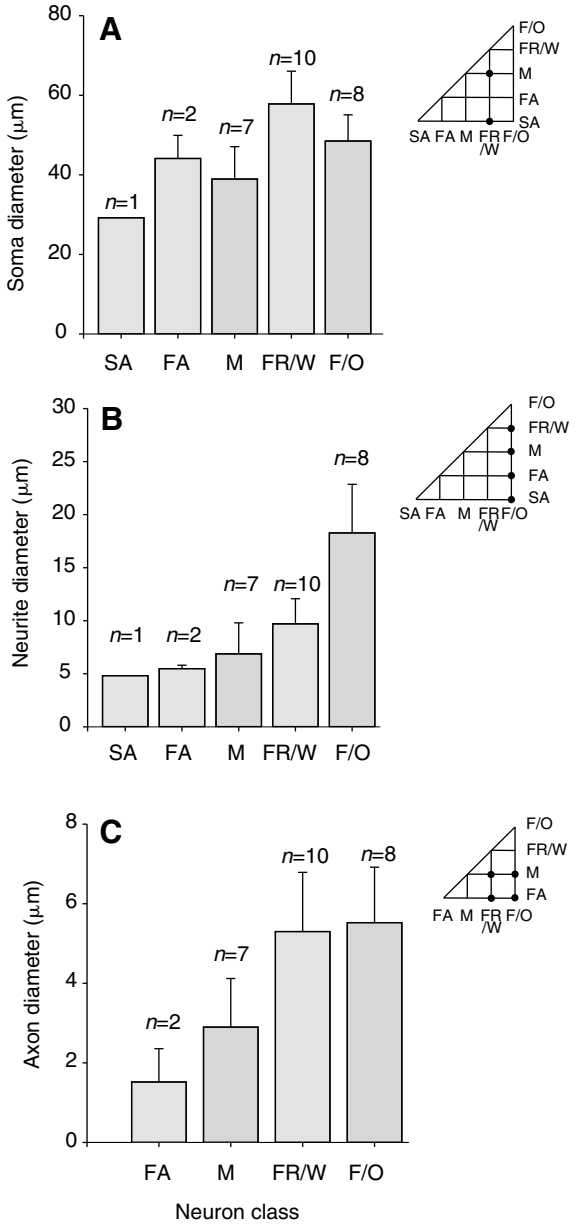

Fig. 14. Soma (A), neurite (B) and axon diameters (C) of the five classes of motor neurons. (A) FR/W class neurons had significantly larger somata than SA and M neurons. Because the somata of these motor neurons were not perfectly round, the diameter was measured by taking the mean of the smallest diameter and the largest diameter. (B) The F/O class neurons had significantly larger neuritic diameters than all other classes of neurons. We measured neurite diameter at the point just posterior to the junction where the neurite from the soma reaches the main branch. (C) FR/W class neurons had significantly larger diameter axons than FA and M class neurons, and F/O class neurons had significantly larger diameter axons than FA and M class neurons. We measured axon diameter at the point where the neurite exits the neuropil. This location is not ideal since the neurites tend to narrow at this point before becoming larger in diameter in the nerve, but unfortunately not all of our dye-fills included the true axon in the nerve.

The finding that there is specificity of chemical synaptic input raises the question of whether or not a similar type of specificity also exists in the electrical connections between the motor neurons (Cattaert et al., 1995). Based on the high degree of heterogeneity found in the present study it would be interesting to measure the strength of electrical coupling between depressor motor neurons of different classes.

Differences between the neuron classes

According to the size principle, neurons with small extracellular spike amplitudes and small soma are recruited before larger neurons. Although we were not able to measure the recruitment order of each class, we looked for systematic differences between the neuron classes related to neuron size. We found that FR/W and F/O class neurons have larger spike amplitudes than all other classes of neurons. This difference in spike amplitude was positively correlated with a difference in the diameter of the axons of these neurons in comparison to the other classes. Despite the small spike amplitude of SA, FA and M class neurons, only the SA neurons had a significantly greater orthodromic delay than all the other neurons. In terms of neurite diameter, only the F/O neurons were significantly larger than the other classes. We also looked at soma diameter but only found differences between FR/W neurons and SA neurons, and between FR/W neurons and M neurons.

A working hypothesis is that the SA, FA and M (MR and MNR) neurons may be relatively low-threshold neurons that respond to sensory input to control posture, whereas the FR/W, FR/O and FNR/O neurons may have higher thresholds for activation and may be used for more rapid and forceful movements.

Why is there a need for a heterogeneous population of motor neurons to control a single muscle?

One answer to the above question is that a certain degree of heterogeneity is necessary for the orderly recruitment of neurons *via* the mechanisms described by the size principle. However, there is an alternative explanation. The size principle works best with a simple muscle with a single origin and insertion. A complex muscle containing more than one origin or insertion may require a specific sequence of activation of motor units that does not strictly follow the rules of the size principle.

In the leg of a decapod crustacean the degree of complexity varies from one muscle to another. In the distal limb within each leg segment, two antagonistic muscles move the next distal segment in opposite directions with movement being restricted to a single plane (Cochran, 1935). In contrast, in the proximal limb, although movement is still restricted to a single plane, the musculature is more complex (Bévengut et al., 1983). Within the proximal limb, functional muscles, defined by the direction of movement they cause, may consist of multiple muscle bundles with multiple origins and insertions (Bévengut et al., 1983). In the crayfish, the depressor muscle consists of two bundles: a rostral bundle with a single origin and a caudal bundle with four origins (Antonsen and Paul, 2000). In order to have smooth movement around the pivot point of the basipodite-coxopodite joint, it is necessary to activate the separate muscle bundles differentially since some will have to contract more in length than others to contribute force equally at the apodeme. Thus, the depressor muscle is complex, and this complexity may require heterogeneity of motor neuron properties and specificity of synaptic input beyond those predicted by the size principle.

Heterogeneity of motor neurons in arthropods

Several studies in invertebrates have shown motor neurons form heterogeneous populations (Bässler, 1989; Millar and Atwood, 2004; Skorupski et al., 1992). For example, in the locust, the nine excitatory motor neurons that innervate the metathoracic flexor tibiae of the hind leg can be divided into three groups: fast, intermediate and slow (Phillips, 1981; Burrows and Hoyle, 1973). They are responsive to different aspects of a sensory stimulus such as position and velocity, as well as slow *versus* fast movements (Field and Burrows, 1982; Newland and Kondoh, 1997).

As in the complex vertebrate muscles (English and Letbetter, 1982), individual invertebrate motor neurons may also innervate a subset of the fibers of a muscle. In the locust, each of the nine motor neurons that innervate the flexor tibia muscle has a distinctive pattern of innervation of muscle fibers (Sasaki and Burrows, 1998).

To conclude, we have found that the population of excitatory neurons that innervate a single muscle of the crayfish leg is very heterogeneous, comprising seven classes of neurons that differ in their anatomical and physiological properties. Whether this heterogeneity serves as a substrate for a relatively simple recruitment scheme, such as that proposed by the size principle, or whether the depressor muscle is more akin to complex vertebrate muscle that require differential activation of muscle compartments, remains to be discovered.

LIST OF ABBREVIATIONS

AL	anterior-lateral
AM	anterior-medial
CBCO	coxo-basipodite chordotonal organ
Dep MN	depressor motor neuron
E	monosynaptic excitatory input
EPSP	excitatory postsynaptic potential
FA	fast assistance
FNR	fast no response
FR	fast resistance
I	inhibitory polysynaptic input
IPSP	inhibitory postsynaptic potential
MNR	medium no response
MR	medium resistance
mvt	movement
O	oblique
P	polysynaptic excitatory input
PL	posterior-lateral
PM	posterior-medial
R	resistance
SA	slow assistance
SR	slow resistance
W	whole neuropile

This work was supported by the Centre National de la Recherche Scientifique (CNRS), and the ACI 'Neurosciences integratives et computationnelles no. 32' from the Ministère de l'Enseignement Supérieur et de la Recherche (France), as well as a Ministere de la Recherche postdoctoral grant to A.A.V.H.

REFERENCES

Antonsen, B. L. and Paul, D. H. (2000). The leg depressor and levator muscles in the squat lobster *Munida quadrispina* (Galatheidae) and the crayfish *Procambarus clarkii* (Astacidae) have multiple heads with potentially different functions. *Brain Behav. Evol.* **56**, 63-85.

Atwood, H. L. (1967). Crustacean neuromuscular mechanism. *Am. Zool.* **7**, 527-551.

Atwood, H. L. and Dorai Raj, B. S. (1964). Tension development and membrane responses in phasic and tonic muscle fibers of a crab. *J. Cell. Comp. Physiol.* **64**, 55-72.

Ballantyne, D. and Rathmayer, W. (1981). On the function of the common inhibitory neurone in the walking legs of the crab, *Eriphia spinifrons*. *J. Comp. Physiol. A* **143**, 111-122.

Barnes, W. J. P. (1977). Proprioceptive influences on motor output during walking in the crayfish. *J. Physiol. Paris* **73**, 543-564.

Bässler, U. (1989). Muscle and reflex partitioning in insects. *Behav. Brain Res.* **12**, 646-647.

Bawa, P., Binder, M. D., Ruenzel, P. and Henneman, E. (1984). Recruitment order of motoneurons in stretch reflexes is highly correlated with their axonal conduction velocity. *J. Neurophysiol.* **52**, 410-420.

Bévengut, M. and Cournil, I. (1990). Gamma-aminobutyric acid-inhibitory motor innervation of leg muscles of the shore crab. *Eur. J. Neurosci.* **2**, 132-139.

Bévengut, M., Simmers, A. J. and Clarac, F. (1983). Central neuronal projections and neuromuscular organization of the basal region of the shore crab leg. *J. Comp. Neurol.* **221**, 185-198.

Binder, B. and Mendel, L. M. (1990). *The Segmental Motor System.* New York: Oxford University Press.

Bullock, T. H. and Horridge, G. A. (1965). *Structure and Function in the Nervous Systems of Invertebrates.* San Francisco: Freeman.

Burke, R. E., Dum, R. P., Fleshman, J. W., Glenn, L. L., Lev-Tov, A., O'Donovan, M. J. and Pinter, M. J. (1982). A HRP study of the relation between cell size and motor unit type in cat ankle extensor motoneurons. *J. Comp. Neurol.* **209**, 17-28.

Burrows, M. and Hoyle, G. (1973). Neural mechanism underlying behavior in the locust *Schistocerca gregaria*. 3. Topography of limb motorneurons in the metathoracic ganglion. *J. Neurobiol.* **4**, 167-186.

Cattaert, D. and Le Ray, D. (2001). Adaptive motor control in crayfish. *Prog. Neurobiol.* **63**, 199-240.

Cattaert, D., Bévengut, M. and Clarac, F. (1993). Synaptic connections between sensory afferents and the common inhibitory motoneuron in crayfish. *J. Comp. Physiol. A* **172**, 71-79.

Cattaert, D., Pearlstein, E. and Clarac, F. (1995). Cholinergic control of the walking network in the crayfish *Procambarus clarkii*. *J. Physiol. (Paris)* **89**, 209-220.

Chrachri, A. and Clarac, F. (1989). Synaptic connections between motor neurons and interneurons in the fourth thoracic ganglion of the crayfish, *Procambarus clarkii*. *J. Neurophysiol.* **62**, 1237-1250.

Clarac, F., Cattaert, D. and Le Ray, D. (2000). Central control components of a 'simple' stretch reflex. *Trends Neurosci.* **23**, 199-208.

Cochran, D. (1935). The skeletal musculature of the blue crab, *Callinectes sapidus* Rathbun. *Smithson. Misc. Coll.* **92**, 1-76.

Davis, W. J. (1969). The neural control of swimmeret beating in the lobster. *J. Exp. Biol.* **50**, 99-117.

Davis, W. J. (1971). Functional significance of motorneuron size and soma position in swimmeret system of the lobster. *J. Neurophysiol.* **34**, 274-288.

Desmedt, J. E. and Godaux, E. (1977). Ballistic contractions in man: characteristic recruitment pattern of single motor units of the tibialis anterior muscle. *J. Physiol. Lond.* **264**, 673-693.
Duysens, J. (1989). Partitionning of reflexes. *Behav. Brain Sci.* **12**, 651.
Duysens, J., Clarac, F. and Cruse, H. (2000). Load-regulating mechanisms in gait and posture: comparative aspects. *Physiol. Rev.* **80**, 83-133.
El Manira, A., DiCaprio, R. A., Cattaert, D. and Clarac, F. (1991). Monosynaptic interjoint reflexes and their central modulation during fictive locomotion in crayfish. *Eur. J. Neurosci.* **3**, 1219-1231.
Elson, R. C. (1996). Neuroanatomy of a crayfish thoracic ganglion: sensory and motor roots of the walking-leg nerves and possible homologies with insects. *J. Comp. Neurol.* **365**, 1-17.
English, A. W. and Letbetter, W. D. (1982). Anatomy and innervation patterns of cat lateral gastrocnemius and plantaris muscles. *Am. J. Anat.* **164**, 67-77.
Field, L. H. and Burrows, M. (1982). Reflex effects of the femoral chordotonal organ upon leg motor neurones of the locust. *J. Exp. Biol.* **101**, 265-285.
Gabriel, J. P., Scharstein, H., Schmidt, J. and Buschges, A. (2003). Control of flexor motoneuron activity during single leg walking of the stick insect on an electronically controlled treadwheel. *J. Neurobiol.* **56**, 237-251.
Henneman, E. (1990). Comments on the logical basis of muscle control. In *The Segmental Motor System* (ed. M. D. Binder and L. M. Mendell), pp. 7-10. New York: Oxford University Press.
Henneman, E. and Mendell, L. M. (1981). Functional organization of motoneuron pool and its inputs. In *Handbook of Physiology, The Nervous System, Motor Control*. Vol. II (ed. V. B. Brooks), pp. 423-507. Bethesda: American Physiological Society.
Henneman, E., Somjen, G. and Carpenter, D. O. (1965). Functional significance of cell size in spinal motoneurons. *J. Neurophysiol.* **28**, 560-580.
Henneman, E., Clamann, H. P., Gillies, J. D. and Skinner, R. D. (1974). Rank order of motoneurons within a pool: law of combination. *J. Neurophysiol.* **37**, 1338-1349.
Kennedy, D. and Davis, W. J. (1977). Organization of invertebrate motor systems. In *Handbook of Physiology.* Vol 1, Part 2 (ed. S. R. Geiger and E. R. Kandel), pp. 1023-1087. Bethesda, MD: American Physiological Society.
Kovac, M. P., Davis, W. J., Matera, E. and Gillette, R. (1982). Functional and structural correlates of cell size in paracerebral neurons of *Pleurobranchaea californica*. *J. Neurophysiol.* **47**, 909-927.
Le Bon-Jego, M. and Cattaert, D. (2002). Inhibitory component of the resistance reflex in the locomotor network of the crayfish. *J. Neurophysiol.* **88**, 2575-2588.
Le Ray, D. and Cattaert, D. (1997). Neural mechanisms of reflex reversal in coxo-basipodite depressor motor neurons of the crayfish. *J. Neurophysiol.* **77**, 1963-1978.
Le Ray, D., Clarac, F. and Cattaert, D. (1997a). Functional analysis of the sensory motor pathway of resistance reflex in crayfish. I. Multisensory coding and motor neuron monosynaptic responses. *J. Neurophysiol.* **78**, 3133-3143.
Le Ray, D., Clarac, F. and Cattaert, D. (1997b). Functional analysis of the sensory motor pathway of resistance reflex in crayfish. II. Integration of sensory inputs in motor neurons. *J. Neurophysiol.* **78**, 3144-3153.
Matsumoto, G. and Tasaki, I. (1977). A study of conduction velocity in nonmyelinated nerve fibers. *Biophys. J.* **20**, 1-13.
Mendell, L. M. (2005). The size principle: a rule describing the recruitment of motoneurons. *J. Neurophysiol.* **93**, 3024-3026.
Millar, A. and Atwood, H. L. (2004). Crustacean phasic and tonic motor neurons. *Integr. Comp. Biol.* **44**, 4-13.
Milner-Brown, H. S., Stein, R. B. and Yemm, R. (1973). Changes in firing rate of human motor units during linearly changing voluntary contractions. *J. Physiol. Lond.* **230**, 371-390.
Newland, P. L. and Kondoh, Y. (1997). Dynamics of neurons controlling movements of a locust hind leg II. Flexor tibiae motor neurons. *J. Neurophysiol.* **77**, 1731-1746.
Petrofsky, J. S. (1978). Control of the recruitment and firing frequencies of motor units in electrically stimulated muscles in the cat. *Med. Biol. Eng Comput.* **16**, 302-308.
Petrofsky, J. S. (1981). The influence of recruitment order and temperature on muscle contraction with special reference to motor unit fatigue. *Eur. J. Appl. Physiol. Occup. Physiol.* **47**, 17-25.
Phillips, C. E. (1981). Organization of motor neurons to a multiply innervated insect muscle. *J. Neurobiol.* **12**, 269-280.
Sasaki, K. and Burrows, M. (1998). Innervation pattern of a pool of nine excitatory motor neurons in the flexor tibiae muscle of a locust hind leg. *J. Exp. Biol.* **201**, 1885-1893.
Skorupski, P., Rawat, B. M. and Bush, B. M. H. (1992). Heterogeneity and central modulation of feedback reflexes in crayfish motor pool. *J. Neurophysiol.* **67**, 648-663.
Wiens, T. J. and Wolf, H. (1993). The inhibitory motoneurons of crayfish thoracic limbs: identification, structures, and homology with insect common inhibitors. *J. Comp. Neurol.* **336**, 261-278.
Zajac, F. E. and Faden, J. S. (1985). Relationship among recruitment order, axonal conduction velocity, and muscle-unit properties of type-identified motor units in cat plantaris muscle. *J. Neurophysiol.* **53**, 1303-1322.
Zajac, F. E., Neptune, R. R. and Kautz, S. A. (2002). Biomechanics and muscle coordination of human walking. Part I: introduction to concepts, power transfer, dynamics and simulations. *Gait Posture* **16**, 215-232.
Zajac, F. E., Neptune, R. R. and Kautz, S. A. (2003). Biomechanics and muscle coordination of human walking. Part II: lessons from dynamical simulations and clinical implications. *Gait Posture* **17**, 1-17.